

Population dynamics of interacting spiking neurons

Maurizio Mattia*

Physics Laboratory, Istituto Superiore di Sanità, INFN - Gr. Coll. Roma I, V.le Regina Elena 299, 00161 Roma, Italy

Paolo Del Giudice†

Physics Laboratory, Istituto Superiore di Sanità, INFN - Gr. Coll. Roma I, V.le Regina Elena 299, 00161 Roma, Italy

(Received 1 October 2001; revised manuscript received 29 March 2002; published 26 November 2002)

A dynamical equation is derived for the spike emission rate $\nu(t)$ of a homogeneous network of integrate-and-fire (IF) neurons in a mean-field theoretical framework, where the activity of the single cell depends both on the mean afferent current (the “field”) and on its fluctuations. Finite-size effects are taken into account, by a stochastic extension of the dynamical equation for the ν ; their effect on the collective activity is studied in detail. Conditions for the local stability of the collective activity are shown to be naturally and simply expressed in terms of (the slope of) the single neuron, static, current-to-rate transfer function. In the framework of the local analysis, we studied the spectral properties of the time-dependent collective activity of the finite network in an asynchronous state; finite-size fluctuations act as an ongoing self-stimulation, which probes the spectral structure of the system on a wide frequency range. The power spectrum of ν exhibits modes ranging from very high frequency (depending on spike transmission delays), which are responsible for instability, to oscillations at a few Hz, direct expression of the diffusion process describing the population dynamics. The latter “diffusion” slow modes do not contribute to the stability conditions. Their characteristic times govern the transient response of the network; these reaction times also exhibit a simple dependence on the slope of the neuron transfer function. We speculate on the possible relevance of our results for the change in the characteristic response time of a neural population during the learning process which shapes the synaptic couplings, thereby affecting the slope of the transfer function. There is remarkable agreement of the theoretical predictions with simulations of a network of IF neurons with a constant leakage term for the membrane potential.

DOI: 10.1103/PhysRevE.66.051917

PACS number(s): 87.10.+e, 05.90.+m, 05.40.-a, 87.19.La

I. INTRODUCTION

The mean-field approach to the analysis of recurrent networks of spiking neurons dates back to the early 1970s; to put our work in perspective, we list a few relevant milestones in this successful history, relevant to the subject of the present paper [1]: One early, seminal work was devoted to the characterization of the frequency response of a homogeneous population of noninteracting integrate-and-fire (IF) neurons in stationary conditions [2]. In Ref. [3], a wider repertoire of dynamical behaviors emerges from an *ad hoc* dynamics introduced for the collective activity of interacting populations of neurons. Building on a well-established knowledge of the stochastic dynamics of a single noise-driven IF neuron, the authors of Ref. [4] could formulate a static mean-field approach taking into account the fluctuation in the external afferent currents in a network context, thus opening the way to the theoretical description of low activity states of interacting IF neurons with high interspike variability. In a tour de force the author of Ref. [5] made an extensive analysis of the mean-field dynamics of populations of interacting IF neurons, incorporating dynamical synaptic currents and adaptation effects (via voltage-independent potassium currents); fluctuations in the afferent currents were not taken into account in Ref. [5]. A complementary analysis was performed in Ref. [6], not including adaptation effects, in

which the local stability conditions were derived for a homogeneous population of IF neurons, also incorporating the effects of a noisy afferent current (independent of the network activity) through a Fokker-Planck formulation. Using an alternative neuron model (the “spike-response” neuron), another approach was built in Ref. [7] to the mean-field dynamics, via the construction of suitable kernels propagating in time the collective activity of a neural population. The theory could accommodate dynamical synaptic currents. The effect of an absolute and/or relative refractory period, fluctuating emission threshold, and a complex dynamical scenario, including asynchronous states and phase locking, was characterized. The mean-field approach was further enriched in Ref. [8], taking into account the fluctuations in the afferent currents self-consistently determined by the network recurrent activity, including excitatory and inhibitory interacting populations and the effects of a Hebbian synaptic structure. A way to incorporate the finite size of the network as a correction to the mean-field formulation was explored in Ref. [9]; a “phase diagram” was derived in this work for an inhibitory network, and the line of bifurcation from stable asynchronous states to high-frequency oscillatory states was calculated by means of a perturbative treatment of a Fokker-Planck formulation. A spectral analysis was performed in Ref. [10] of the collective activity of a single population of (excitatory or inhibitory) neurons of the “spike-response” type, taking into account the finite size of the network in a way similar to Ref. [9], but without considering noisy currents.

With somewhat different motivations, an approach was

*Electronic address: mattia@iss.infn.it

†Electronic address: paolo.delgiudice@iss.infn.it

proposed in Ref. [11] to the numerical solution of the above Fokker-Planck formulation of the network dynamics, which involves expanding the Fokker-Planck operator onto a time-dependent basis.

Motivated by a dynamical description of the mean-field theory, we use a similar formalism which, complemented by the appropriate “self-consistency” ingredients, allows us to formulate in closed form dynamical equations for the fraction of neurons spiking per unit time $\nu(t)$ (the “collective activity” or “emission rate” of the neural population in the following) in the presence of noise.

With this approach, we could reproduce in a unified frame several key results of the works quoted above, but new qualitative and quantitative features also emerge. (i) From an approximate solution of the dynamical equations for ν , a peculiar role emerges for the single neuron response properties; this, in our view, is a step forward in the long-standing problem of relating single neuron properties to the collective activity of interacting assemblies of neurons [2,5,6,8,7]. (ii) Taking in due consideration the fact that neurons only communicate with each other via spikes led us to reformulate the way in which finite-size noise enters the Fokker-Planck description of the collective dynamics; this generates additional features in the spectral content of the collective activity, with respect to those already observed in Refs. [10,9]. (iii) Our formalism encompasses in a natural way the description of neural populations operating in a *noise-dominated* (sub-threshold) regime, recognized to be relevant for the description of neural activity characterized by low emission rates and high variability in the interspike intervals [8,12,13]. We show that a characteristic low-frequency behavior of the population frequency response, and a peculiar hierarchy of characteristic times of the population transient response, emerge. (iv) With a focus on the asynchronous collective states (which are widely recognized as representative of typical cortical conditions), it turns out that the response times of the neural population to sharp variations in the input, besides being strongly affected by noise, are remarkably sensitive to the intensity of the average synaptic couplings. This foreshadows a link between the latency of the response to a stimulus and a “learning” process having taken place in the network. The asynchronous states provide a natural, fast vehicle to propagate the information flow, as previously suggested in various contexts [2,5,14,15] (see also [16] for an experimental estimate of the speed of processing in the visual cortex).

In the first part of the paper, after briefly reviewing the “population density approach,” we illustrate the general formalism that allows us to write a dynamical equation for the collective activity of a population of generic IF neurons. A linearized analysis follows, which allows us to study the local stability for the asynchronous states and the characteristic times of the transient network response. We then turn to the analysis of the finite-size effects and the power spectral density of the network activity. In the second part we turn to a specific example application of the general theory, studying the mean-field dynamics of a network of IF neurons with constant leakage term (the “linear” neuron studied in Ref. [12]), and a detailed comparison is performed between the

theoretical predictions and numerical simulations.

II. A GENERAL APPROACH

A. Single neuron equation

A generic integrate-and-fire (IF) neuron can be fully described by the following dynamics of its membrane potential $V(t)$ (depolarization):

$$\dot{V} = f(V) + I(V, t)/C, \quad (2.1)$$

where $f(V)$ is the deterministic drift towards a resting potential [$f(V) = -V/\tau$, leaky IF neuron; $f(V) = -\beta$, constant leakage, linear IF neuron (LIF) [12]], C is an effective cell membrane capacitance, and $I(V, t)$ is the ionic current due to incoming spikes from the presynaptic neurons through the dendritic contacts, and can be adequately modeled, for a realistic number of presynaptic afferents (connectivity), as a superposition of stochastic, independent point processes. When $V(t)$ crosses a threshold θ , the neuron emits an action potential (the spike) with an infinitesimal time duration, and the depolarization is instantaneously reset to a value H .

Under reasonable assumptions, including the diffusion approximation, the limit of a large number of afferents, and the independence between the activities of the presynaptic cells (see the detailed discussion in Ref. [17]), the afferent current $I(V, t)$ is well described by a (possibly nonstationary) Wiener process and the dynamics of the neuron’s membrane potential is governed by the following nonlinear Langevin equation:

$$\dot{V} = h(V, t) + \sigma(V, t)\Gamma(t), \quad (2.2)$$

where $h(V, t)$ is the total deterministic drift [sum of $f(V)$ and the average afferent current $\mu(V, t) = \langle I(V, t)/C \rangle$]; $\sigma(V, t) = \sqrt{\langle [I(V, t)/C - \mu(V, t)]^2 \rangle}$, the size of current fluctuation, i.e., the variance of the afferent current. $\Gamma(t)$ is a δ -correlated (*white*) noise with zero mean and unitary variance. $\langle \rangle$ above denotes averaging with respect to the probability distribution of the process at time t .

The emission of a spike and the limits on the accessible values for the depolarization can be taken into account by suitable boundary conditions for the stochastic differential equation (2.2), as we discuss later in more details.

B. The dynamics of a single neural population

For a large homogeneous network of N interacting IF neurons, the mean-field approximation [8] assumes the same statistical properties μ and σ^2 for the afferent currents to the N cells. The N depolarizations V are considered as N independent realizations of the stochastic process (2.2), whose properties are described by a (time-dependent) probability density function (p.d.f.) $p(v, t)$ [18]. The above independence assumption (to be checked *a posteriori*) allows us to use the percentage of neurons having $V(t) \in [v, v + dv]$ as an estimate of $p(v, t)dv$. The evolution of $p(v, t)$ is described by the following Fokker-Planck equation:

$$\partial_t p(v, t) = Lp(v, t), \quad (2.3)$$

where L is the differential Fokker-Planck operator, which takes the general form

$$L(v,t) = -\partial_v A(v,t) + \partial_v^2 B(v,t). \quad (2.4)$$

The $A(v,t)$ term is the drift coefficient and $B(v,t)$ is the diffusion coefficient of the stochastic process $V(t)$. Equation (2.3), with its boundary conditions, fully describes the population dynamics. The A and B coefficients can be derived from Eq. (2.2) and are

$$A(v,t) = f(v) + \mu(v,t) = h(v,t),$$

$$B(v,t) = \frac{1}{2} \sigma^2(v,t)$$

(see Refs. [19,20]).

Equation (2.3) can be regarded as a *continuity equation*

$$\partial_t p(v,t) = -\partial_v S_p(v,t),$$

where $S_p(v,t)$ is the net flux of realizations (or ‘‘probability current’’) crossing the level v at time t . Its explicit form is

$$S_p(v,t) = [A(v,t) - \partial_v B(v,t)]p(v,t).$$

The depolarization is assumed to vary between v_{\min} and θ , including the possibility that $v_{\min} \rightarrow -\infty$.

In particular, the fraction of realizations per unit time crossing the threshold θ , i.e., the average neuron emission rate $\nu(t)$ in the population, is given by the flux

$$\nu(t) \equiv S_p(\theta,t).$$

θ acts as an *absorbing barrier*, such that

$$p(\theta,t) = 0, \quad (2.5)$$

and the emission rate becomes

$$\nu(t) = -B(v,t)\partial_v p(v,t)|_{v=\theta} = -\frac{1}{2}\sigma^2(v,t)\partial_v p(v,t)|_{v=\theta}. \quad (2.6)$$

An equivalent, operational definition of the population rate for a finite number N of neurons is

$$\nu(t) = \lim_{\Delta t \rightarrow 0} \frac{\mathcal{N}(t,t+\Delta t)}{N\Delta t},$$

where $\mathcal{N}(t,t+\Delta t)$ is the total number of spikes emitted by the population in the time interval $(t,t+\Delta t)$.

Realizations crossing the threshold restart their random walk from $v=H$, after a refractory period of inactivity τ_0 , and this implies the following conservation of the net flux $S_p(v,t)$:

$$S_p(\theta,t-\tau_0) = S_p(H^+,t) - S_p(H^-,t), \quad (2.7)$$

where $S_p(H^\pm,t) = \lim_{v \rightarrow H^\pm} S_p(v,t)$.

A *reflecting barrier* prevents V from going below v_{\min} , and this implies a vanishing probability current through v_{\min} ,

$$S_p(v_{\min},t) = 0. \quad (2.8)$$

In the mean-field approach, the infinitesimal moments of the afferent current are expressed as functions of $\nu(t)$ [8,12], now interpreted as the emission rate of presynaptic neurons,

$$\mu(v,t) = \mu[v,\nu(t)],$$

$$\sigma^2(v,t) = \sigma^2[v,\nu(t)].$$

Closing this loop makes the Fokker-Planck equation (2.3) nonlinear, because the infinitesimal moments depend on the emission rate $\nu(t)$ and therefore on the system state, so that $L=L(p)$.

We also mention that a population density approach is viable also when the diffusion approximation is not valid (see [21]).

C. Eigenfunction analysis

The Fokker-Planck operator (2.4) has a set of eigenfunctions and associated eigenvalues,

$$L|\phi_n\rangle = \lambda_n(t)|\phi_n\rangle. \quad (2.9)$$

Defining the inner product

$$\langle\psi|\phi\rangle = \int \psi(v,t)\phi(v,t)dv,$$

the adjoint operator L^+ ,

$$\langle\psi|L\phi\rangle = \langle L^+\psi|\phi\rangle, \quad (2.10)$$

has eigenfunctions $|\psi_m\rangle$ and eigenvalues $\tilde{\lambda}_m$ that are in general different from those of L , because L is not Hermitian. In the above expressions, the time dependence is implicitly due to the time dependence of μ and σ^2 . The boundary conditions for ψ and the expression for L^+ can be derived from the boundary conditions for the ϕ [19,11].

Assuming ϕ_n is a complete set of eigenfunctions, the boundary conditions (2.5), (2.7), and (2.8) must be satisfied by each $\phi_n(v,t)$.

The following conditions on the eigenfunctions ψ_n of L^+ result:

$$\psi_n(\theta,t)S_{\phi_n}(\theta,t) = \psi_n(H,t)S_{\phi_n}(\theta,t-\tau_0),$$

$$\partial_v \psi_n(v_{\min},t) = 0,$$

$$\partial_v \psi_n(H^+,t) = \partial_v \psi_n(H^-,t),$$

assuming ψ_n and ϕ_n to be continuous functions in the interval (v_{\min},θ) .

The adjoint operator is then given by

$$\begin{aligned} L^+(v,t) &= A(v,t)\partial_v + B(v,t)\partial_v^2 \\ &= [f(v) + \mu(v,t)]\partial_v + \frac{1}{2}\sigma^2(v,t)\partial_v^2, \end{aligned} \quad (2.11)$$

which is the evolution operator for the backward Kolmogorov equation, completely equivalent to Eq. (2.3).

Equation (2.10) implies that eigenfunctions with different eigenvalues are orthogonal; for the completeness assumption of the eigenfunctions of the Fokker-Planck operator,

$$\mathbf{I} = \sum_n |\phi_n\rangle\langle\psi_n|, \quad (2.12)$$

both L and L^+ have the same eigenvalues ($\lambda_m = \tilde{\lambda}_m$), and with an appropriate normalization the two sets of eigenfunctions are biorthonormal,

$$\langle\psi_n|\phi_m\rangle = \delta_{nm}. \quad (2.13)$$

For simplicity, we will neglect the refractory period τ_0 in the following, considering $\tau_0=0$ as a good approximation for not too high spike emission rates ($\nu \ll 1/\tau_0 \approx 500$ Hz).

1. Some remarks on eigenvalues and eigenfunctions

We list below some general properties of the eigenvalues and eigenfunctions of L which will be instrumental in the following; we will sometimes use the case of noninteracting neurons as an easy reference situation for illustrative purposes, although the statements in this subsection apply to the general, interacting case.

$\lambda_0=0$ is always an eigenvalue of L , and the corresponding eigenfunction ϕ_0 is the stationary solution of the population dynamics: $\partial_t \phi_0 = 0$.

The eigenvalues are in general complex, with $\text{Re } \lambda_n \leq 0$, $\forall n \neq 0$, [22]; the latter condition can be inferred from the fact that, for an ensemble of noninteracting neurons, the solution of the Fokker-Planck equation is directly related to the eigenvalues of L , and is expected to converge to ϕ_0 , instead of exploding, which would be the case for positive eigenvalues (see also Sec. IID 1).

If λ_n is an eigenvalue, also λ_n^* is an eigenvalue, with eigenfunction $|\phi_n^*\rangle$ ($\langle\psi_n^*|$), because $L(L^+)$ is real. We set $\lambda_{-n} = \lambda_n^*$ and consequently $|\phi_{-n}\rangle = |\phi_n^*\rangle$, so that the sums over the spectrum of the Fokker-Planck operator range over all the integer numbers. Obviously if $\lambda_n \in \mathbb{R}$, the enumeration along the negative values of n is redundant, and we will see later how this is handled in a specific example.

From the form of L^+ , and the boundary condition $\partial_v \psi_n(v_{\min}, t) = 0$, it can be seen that the eigenfunction ψ_0 must always satisfy the condition $\partial_v \psi_0 = 0$, so ψ_0 is a constant. Because $\langle\psi_0|\phi_0\rangle = 1$ and $\phi_0(v)$ is a p.d.f., so that

$$\int_{v_{\min}}^{\theta} \phi_0(v) dv = 1,$$

we have $\psi_0 = 1$. Finally, using Eq. (2.13),

$$\langle\psi_0|\phi_n\rangle = \int_{v_{\min}}^{\theta} \phi_n(v) dv = 0, \quad \forall n \neq 0. \quad (2.14)$$

From this result we can argue that only the stationary mode ϕ_0 contributes to the normalization condition for $p(v, t)$ (see also [22]). As we will see later, this is a useful feature of the eigenfunction expansion [11].

When the mean driving force alone is not enough to make V cross the threshold θ [$A(\theta, t) \leq 0$], so that a positive diffusion term is necessary to have the emission of a spike, the neurons are evolving in a *noise-dominated, subthreshold* regime, whereas when $A(\theta, t) > 0$, the emission of an action potential can occur also in the absence of noisy afferent currents, and the neurons are in a *drift-dominated, suprathreshold* regime of activity [8,23,12,9,13]. The activity regime characterizes the statistical properties of the single neuron spike train: irregular firing (high coefficient of variation [24]) corresponds to a noise-dominated regime, while regular spike trains are related to a drift-dominated regime. Such a spread in the coefficient of variation of interspike intervals of the single neuron does not spoil the hypothesis of the theory, as long as the independence of the firing of different neurons holds [12,13], which is reasonable in biologically plausible conditions [25].

We conjecture that the eigenvalues of L are real for noise-dominated regimes and complex conjugates for drift dominated regimes. For an ensemble of noninteracting neurons, whose dynamics is directly driven by the eigenvalues of L , this implies that for drift-dominated regimes the neural noninteracting population can undergo transient oscillations (on the way to the stationary state), while this would be forbidden for noise-dominated regimes.

The above statements have been confirmed by explicit calculation in the case of constant A and B (Wiener process with drift, “linear IF neuron”), to be discussed in Sec. III.

As an aid to intuition, one can think of a $p(v, t)$ which is initially very sharply concentrated; if the dynamics of p is essentially governed by the drift A , its motion along the allowed domain $[v_{\min}, \theta]$ is close to a translation, with a minor spreading effect due to diffusion. The probability flux across θ is zero until the upper tail of p reaches θ , increases as the bulk of the distribution goes through θ , and vanishes again. From then on, p restarts traveling from v_{\min} to θ , while maintaining slow spreading, and the emission rate undergoes increasingly damped oscillations, until the stationary state is reached. As a toy example of an alternative case, one can imagine a pure diffusion (zero drift) process, starting from the same initial condition, which even in the case of a v -dependent B makes p spread more and more, without igniting oscillations.

Although the above examples are special and simple, it seems reasonable to assume that (transient) oscillations are possible only when some “memory” is present in the motion of p , and this can only be associated with the drift term.

As we show later, the eigenvalues of L are not simply related to the characteristic times of the system in the presence of a recurrent interaction, and the network activity can be oscillatory also in the noise-dominated regime.

D. The emission rate equation

Thanks to the completeness relation (2.12), $p(v, t)$ can be expressed as

$$|p\rangle = \sum_n a_n |\phi_n\rangle, \quad (2.15)$$

where $a_n = \langle \psi_n | p \rangle$ are the time-dependent coefficients of the modal expansion. Since p is real, $a_n^* = a_{-n}$.

The dynamics of the a_n can be determined directly from the Fokker-Planck equation (2.3) (see, for instance, Ref. [11]),

$$\begin{aligned} \dot{a}_n &= \langle \psi_n | \partial_t p \rangle + \langle \partial_t \psi_n | p \rangle = \langle \psi_n | L p \rangle + \sum_m a_m \langle \dot{\nu} \partial_\nu \psi_n | \phi_m \rangle \\ &= \langle L^+ \psi_n | p \rangle + \dot{\nu} \sum_m a_m \langle \partial_\nu \psi_n | \phi_m \rangle \end{aligned}$$

and then

$$\dot{a}_n = \lambda_n a_n + \dot{\nu} \sum_m a_m \langle \partial_\nu \psi_n | \phi_m \rangle. \quad (2.16)$$

Here we have used the fact that the only time dependence of ψ is implicitly due to the moments of the current, μ and σ^2 , which are in turn functions of the rate $\nu(t)$ (in other words, external input is assumed to be stationary). If several populations are present, $\partial_t \psi$ will have contributions from the emission rates of the different populations (see Sec. II G), including external neurons, and $\langle \partial_\nu \psi_n | \phi_m \rangle$ should be regarded as a *population coupling term*; it vanishes if ν does not enter the afferent current and does not affect the dynamics of the depolarizations.

The infinite set of nonlinear differential equation (2.16) does not contain all the information on the dynamics of the system. What is missing is the answer to the following question: Which is the emission rate ν , given $p(v, t)$? To “close the loop” and generate closed equations for the a (or the ν , which is the natural observable for the collective state of the neural population) one needs a relation connecting $p(v)$ to ν . ν is the flux across the absorbing barrier which, from Eqs. (2.6) and (2.15), is

$$\nu = -\frac{1}{2} \sum_n a_n \sigma^2(v, t) \partial_\nu \phi_n(v, t) |_{v=\theta}. \quad (2.17)$$

Equations (2.16) and (2.17) describe completely the dynamics of the neural population, using as the only observable describing the system the probability current across the threshold: the instantaneous emission rate ν . This is an effective way to reduce the dimensionality of the problem because, as we will see later, a finite (and small) number of a s is often enough for an adequate description of the time evolution of ν [26].

The following remarks provide a simplification. Because only the stationary mode contributes to the normalization condition of $p(v, t)$, it follows that $a_0 = 1$ at all times. Since $\psi_0 = 1$, the coupling term $\langle \partial_\nu \psi_0 | \phi_m \rangle = 0$. Furthermore, the flux due to the stationary mode ϕ_0 is the current-to-rate transduction function $\Phi(\mu, \sigma^2)$ of the single neuron in stationary conditions [12],

$$\Phi(\nu) = \Phi(\mu(v, \nu), \sigma^2(v, \nu)) = -\frac{1}{2} \partial_\nu \sigma^2(v, t) \phi_0(v, t) |_{v=\theta},$$

which binds the single neuron properties to the population dynamics.

The (nonlinear) emission rate equation system can be written in matrix form as

$$\begin{aligned} \dot{\vec{a}} &= (\mathbf{\Lambda} + \mathbf{C} \dot{\nu}) \vec{a} + \vec{c} \dot{\nu}, \\ \nu &= \Phi + \vec{f} \cdot \vec{a}, \end{aligned} \quad (2.18)$$

where \vec{a} is the vector of the modal expansion coefficients with $n \neq 0$; the elements of \vec{f} are the flux over the absorbing barrier for nonstationary modes [27],

$$f_n = -\frac{1}{2} \partial_\nu \sigma^2(v, t) \phi_n(v, t) |_{v=\theta}, \quad \forall n \neq 0, \quad (2.19)$$

the elements of \vec{c} are the coupling terms between the n th mode and the stationary one,

$$c_n = \langle \partial_\nu \psi_n | \phi_0 \rangle, \quad \forall n \neq 0,$$

while \mathbf{C} is the matrix of the coupling terms between the nonstationary modes

$$C_{nm} = \langle \partial_\nu \psi_n | \phi_m \rangle, \quad \forall n, m \neq 0.$$

$\mathbf{\Lambda}$ is a diagonal matrix whose elements are the eigenvalues of L ,

$$\Lambda_{nm} = \lambda_n \delta_{nm}, \quad \forall n, m \neq 0.$$

Under the hypotheses which define the mean-field approximation, Eq. (2.18) describes the collective behavior of a pool of neurons in terms of the fraction of emitting neurons per unit time, $\nu(t)$, thus providing a dynamical formulation of the mean-field treatment, equally valid in stationary or transient regimes [28].

A nonstationary $\nu(t)$ embodies the changes in time of the average statistical properties of the neurons' afferent current, and can correlate the activities of two given neurons; this should be regarded as a “trivial” correlation due to the input part of the current that neurons have in common (self-consistently taken into account in the above mean-field treatment). This does not imply a breakdown of the *independence* hypothesis which is at the heart of the formalism. The collective activity is still adequately described by a renewal, nonstationary Poisson process completely determined by ν : Neurons are independent, conditionally to the average emission rate.

We also remark that μ and σ^2 in the network are no longer independent parameters, but are linked through ν , such that the latter becomes a *complete* description of the network dynamics in the mean-field approximation.

1. Noninteracting neurons

A very simple case is that of a population of noninteracting neurons. Since μ and σ^2 do not depend on ν , $\partial_\nu \psi_n = 0$ and the coupling terms vanish ($\mathbf{C} = 0$ and $\vec{c} = 0$). The emission rate equation (2.18) has now an explicit solution,

$$\nu(t) = \Phi(\mu(t), \sigma^2(t)) + \vec{f}(t) \cdot e^{\int_0^t \Lambda(t') dt'} \vec{a}(0).$$

As the afferent current is stationary, the eigenvalues, the flux vector, and the transfer function are constants and the emission rate is

$$\nu(t) = \Phi(\mu, \sigma^2) + \sum_n f_n a_n(0) e^{\lambda_n t} \quad (2.20)$$

so that the spectrum of L determines directly the characteristic times of the population dynamics (the same result for the uncoupled network is reported in [22]). Consistently with previous remarks, as $t \rightarrow \infty$, $\nu \rightarrow \Phi(\mu, \sigma^2)$, coherently with a negative real part of the eigenvalues.

For $\text{Re } \lambda_n < 0$, after a time greater than $1/\min_n |\text{Re } \lambda_n|$, initial conditions and transients are forgotten, and the stationary population activity is the same as the mean-field rate emission $\Phi(\mu, \sigma^2)$ of the single neurons.

When the interaction is turned on, the ‘‘population characteristic times’’ are obviously a complex mixture of single neuron properties and the properties of the collective activity.

2. Synaptic delays

If we consider a constant delay time δ in the transmission of spikes, the rate equation is modified because all the terms including the parameters of the input currents [$\mu(v, t)$ and $\sigma^2(v, t)$, implicit functions of ν] are to be calculated at time $t - \delta$,

$$\begin{aligned} \dot{\vec{a}}(t) &= [\mathbf{\Lambda}(t - \delta) + \mathbf{C}(t - \delta) \dot{\nu}(t - \delta)] \vec{a}(t) \\ &+ \vec{c}(t - \delta) \dot{\nu}(t - \delta), \end{aligned} \quad (2.21)$$

$$\nu(t) = \Phi(t - \delta) + \vec{f}(t - \delta) \cdot \vec{a}(t).$$

We can in principle generalize to the case in which delays are drawn randomly and independently at each site from a distribution $\rho(\delta)$. We should then take δ into account in the causal agent, the average number of afferent spikes per unit time (ν), substituting every occurrence of $\nu(t - \delta)$ with $\int \nu(t - \delta) \rho(\delta) d\delta$ [9].

E. Local analysis

The fixed points of the autonomous system (2.21) are given by $\dot{\vec{a}} = 0$ and $\dot{\nu} = 0$,

$$\begin{aligned} \vec{a} &= 0, \\ \nu &= \Phi(\nu). \end{aligned} \quad (2.22)$$

This is the self-consistency equation introduced in Ref. [4], and used in the context of a mean-field treatment in Ref. [8] to study the steady states of a network of IF neurons. As expected, the condition $\vec{a} = 0$ implies that the p.d.f. of the depolarization at the fixed point is the stationary mode [$p(v) = \phi_0(v)$].

With a time-dependent perturbation approach we can study the local stability of the fixed points, their nature, and

the characteristic times of transient departures from them. To start, we set $\vec{a} = \varepsilon \vec{a}_1 + \varepsilon^2 \vec{a}_2 + \dots$ and $\nu = \nu_0 + \varepsilon \nu_1 + \varepsilon^2 \nu_2 + \dots$, where ν_0 is the solution of the self-consistency equation (2.22) and ε is the size of the perturbation from the fixed point. Any function F of ν can be expanded as a Taylor’s series, which to second order gives

$$\begin{aligned} F(\nu) &= F(\nu_0) + \varepsilon F'(\nu_0) \nu_1 + \varepsilon^2 [F'(\nu_0) \nu_2 + \frac{1}{2} F''(\nu_0) \nu_1^2] \\ &+ \dots, \end{aligned}$$

where $F' = \partial_\nu F$.

Inserting the above expansion in the rate equation, and comparing the terms of the same order, the dynamics of the first-order perturbation is

$$\begin{aligned} \dot{\vec{a}}_1(t) &= \mathbf{\Lambda}(\nu_0) \vec{a}_1(t) + \vec{c}(\nu_0) \dot{\nu}_1(t - \delta), \\ \nu_1(t) &= \Phi'(\nu_0) \nu_1(t - \delta) + \vec{f}(\nu_0) \cdot \vec{a}_1(t). \end{aligned}$$

This system of ordinary differential equations with constant coefficients can be solved using the Laplace transform. The resulting transformed emission rate $\nu_1(s)$ is

$$\begin{aligned} \nu_1(s) &= \frac{1}{(e^{s\delta} - \Phi') - \vec{f} \cdot (s\mathbf{I} - \mathbf{\Lambda})^{-1} \vec{c}s} \{ \vec{f} \cdot (s\mathbf{I} - \mathbf{\Lambda})^{-1} \\ &\times [\vec{a}_1(0) e^{s\delta} + \vec{c} \nu_1(0)] - (e^{s\delta} - 1) \Phi' \nu_1(0) / s \}, \end{aligned} \quad (2.23)$$

where $(s\mathbf{I} - \mathbf{\Lambda})^{-1}$ is a diagonal matrix with elements $1/(s - \lambda_n)$ and all the functions of ν are evaluated at $\nu = \nu_0$. In performing the Laplace transform of ν_1 and \vec{a} , we assumed $\vec{a}_1(t) = \vec{a}_1(0)$ and $\nu_1(t) = \nu_1(0)$ for any $t < 0$.

The stability conditions and the characteristic times of the transient dynamics are in principle derived by standard methods, by calculating the poles of $\nu_1(s)$. To characterize the poles, we resort to approximations; we will see in the following two subsections how two kinds of small-coupling approximation allow us to characterize two sets of poles of $\nu_1(s)$, which expose very different dynamical features.

We notice that, in order to find the whole set of poles of $\nu_1(s)$, only the zeros of $(e^{s\delta} - \Phi') - \vec{f} \cdot (s\mathbf{I} - \mathbf{\Lambda})^{-1} \vec{c}s$ are needed: the other two possibly contributing terms which appear in the curly brackets do not actually contribute [29].

I. Stability

The asynchronous state $\nu(t) = \nu_0$ is stable if all the poles s_n of $\nu_1(s)$ have a negative real part. To evaluate the stability conditions, we first look for poles on the imaginary axes, which (if they exist) separate the region of stability from that of instability. The poles $s_n = x_n + iy_n$ of $\nu_1(s)$ solve the equations

$$\begin{aligned} e^{x\delta} \cos(y\delta) - R(s) &= \Phi', \\ e^{x\delta} \sin(y\delta) - I(s) &= 0, \end{aligned} \quad (2.24)$$

where $R(s) = \text{Re}[\vec{f} \cdot (s\mathbf{I} - \mathbf{\Lambda})^{-1} \vec{c}s]$, $I(s) = \text{Im}[\vec{f} \cdot (s\mathbf{I} - \mathbf{\Lambda})^{-1} \vec{c}s]$, and $s = x + iy$. Due to the presence of the \vec{c} terms, $R(s)$ and $I(s)$ are expressions of the recurrent coupling and vanish for uncoupled neurons.

The solutions are quite different depending on the excitatory or inhibitory nature of the neurons. For a population of excitatory neurons, Φ is a monotonically increasing function of ν , $\Phi'(\nu) > 0$. In the case $\Phi'(\nu_0) = 1$, it is easy to see that $s = 0$ is a real pole of $\nu_1(s)$. This exact condition determines a transition from stable to unstable steady states for the system, because when

$$\Phi'(\nu_0) > 1,$$

the real pole becomes positive and ν_0 is an unstable state [30]. We can see this by taking as an approximation of this real pole the solution of $e^{s\delta} - \Phi' = 0$,

$$s_0 = \frac{1}{\delta} \ln \Phi'(\nu_0), \quad (2.25)$$

which is indeed a good approximation if the real pole is close to zero [$|s| \ll \min|\text{Re}(\lambda_n/f_n c_n)|$].

To characterize one set of solutions of Eqs. (2.24), we assume that for sufficiently small coupling the terms $R(s)$ and $I(s)$ are negligible compared to Φ' , at least in the neighborhood of a point $s_n^{(0)}$ which is a solution of

$$\begin{aligned} e^{x\delta} \cos(y\delta) &= \Phi', \\ e^{x\delta} \sin(y\delta) &= 0, \end{aligned} \quad (2.26)$$

and is given by $s_n^{(0)} = (\ln \Phi' + i2n\pi)/\delta$ for excitatory neurons and $s_n^{(0)} = [\ln|\Phi'| + i(2n-1)\pi]/\delta$ for inhibitory neurons (n runs over the integers).

Under the above assumption, to be checked *a posteriori*, we can perturbatively expand around $s_n^{(0)}$ (with respect to $|R + iI|$) to find a succession of solutions of Eqs. (2.24),

$$s_n = s_n^{(0)} + \frac{\vec{f} \cdot (s\mathbf{I} - \mathbf{\Lambda})^{-1} \vec{c}s|_{s=s_n^{(0)}}}{\Phi' \delta}.$$

Such poles cross the imaginary axis and destabilize the asynchronous state when $\text{Re } s_n = 0$. This happens when

$$\Phi' \simeq 1 - R(i2\pi n/\delta)$$

for excitatory neurons, and when

$$\Phi' \simeq -1 - R[i(2n-1)\pi/\delta].$$

for inhibitory neurons (the stability condition in this case is approximately given by $\Phi' > -1$).

In the cases examined in the following, it turns out that the poles s_n move towards the imaginary axis for increasing $|\Phi'|$, and for excitatory neurons the pole on the real axis is the first to reach the imaginary axis.

For drift-dominated regimes, the above results hold provided that s_n is far from λ_n , because otherwise $R(s)$ and $I(s)$ are no longer negligible; since $\text{Im } \lambda_n \sim \nu_0$ [6,22] and

$\text{Im } s_n \sim 1/\delta$, the above condition is certainly satisfied if $\delta \ll 1/\nu_0$, which is the case in the typical frequency range.

A noteworthy implication of the above stability analysis is that a *single neuron* feature, the slope of the current-to-rate transduction function Φ , determines in general the stability of the fixed point ν_0 for a *population* of neurons. It is also worth noting that Φ' depends on the synaptic coupling strengths, via μ and σ^2 , and the average properties of the recurrent interaction among neurons emerge as the primary features governing the network stability.

We also remark that the above stability condition, being derived in the framework of the linear analysis, depends on the dynamics (2.1) of the single neuron membrane potential v only through ν (via μ and σ^2). Indeed, in the linear approximation we can write the evolution equation for ν in such a way that the a no longer appear. It is tempting to speculate that, even in the nonlinear case of Eq. (2.18), since the time evolution of $p(v, t)$ is ultimately determined by ν through μ and σ^2 , the dynamics of the probability current ν is in fact a complete description of the dynamics of $p(v, t)$ (once initial conditions and stationary external input are given). The seemingly nonrecoverable loss of information which takes place when reducing the motion of $p(v, t)$ to that of $\nu(t)$ could be avoided because of the peculiar dependence of the Fokker-Planck equation on the ν itself; a related concept will be touched upon in Sec. II F, where we emphasize that different “histories” $V(t)$ in the ensemble described by $p(v, t)$ only communicate to each other via spikes.

The infinite set of poles responsible for the stability of the system are due to the presence of a delay δ in the transmission of the spikes: we therefore call them *transmission poles* $s_n^{(t)}$. For a system close enough to the stability boundary, very high frequency of activity at frequencies of order $1/\delta$ can arise. Transmission poles disappear for uncoupled neurons.

As will become clearer in the following, those oscillations, fast as they are, have nothing to do with the possible slow, oscillatory response of the network to a change in its external inputs.

This set of poles was first observed in a mean-field approach not taking into account fluctuations in the afferent current in Ref. [5], where they are termed the *gross structure* of the spectrum. Furthermore, previous works by other authors [9,31,13] have shown that the description of the system beyond the stability boundary is described (once a third-order expansion has been carried out) by very fast limit cycles, at least for networks of inhibitory IF neurons. On the other hand, Eq. (2.24) provides a generalization of the findings of the quoted works as for the dynamics within the stability region.

Coming back to the role of delays, it turns out that for an excitatory population in drift-dominated regimes, the real part of $s_n^{(t)}$, as a function of δ , for fixed Φ' is not monotonic for large δ (contrary to what happens in the approximations adopted above). For successive values of n , $\text{Re } s_n^{(t)}$ becomes positive in an interval of values of δ , and different n correspond to intervals beginning at $\delta \sim n/\nu_0$. Thus, for large delays the instability of the excitatory network with negligible

noise can be oscillatory in nature. The dynamical scenarios emerging in such situations has been described in [15]. For large delays, the oscillatory instability which occurs at frequencies near $\text{Im} \lambda_m$ is driven by a transmission pole $s_k^{(t)}$ close to the diffusion pole $s_m^{(d)}$. So a kind of coupling emerges in this condition between the transmission and the diffusion poles: the almost regular transport of realizations with approximate periodicity $1/\nu_0$ locks to the transmission of waves of neural activity, affected by a delay $\delta \sim 1/\nu_0$ [7,32].

2. Transient behavior and characteristic times

We remarked that for uncoupled neurons, the poles of ν_1 are the eigenvalues of the Fokker-Planck operator. This suggests a guess for finding other sets of poles as small-coupling perturbations of the λ . For the sake of a clear presentation, we consider the case of a population of excitatory neurons in a drift-dominated regime, and we focus on the first eigenvalue, λ_1 (and its complex conjugate), assuming $|s| \delta \ll 1$ such that $e^{s\delta} \approx 1 + s\delta$ (verified *a posteriori* to be a very good approximation for physiologically reasonable values of synaptic delays). We also assume that the terms $f_n c_n s / (s - \lambda_n)$ are negligible for $n \neq \pm 1$. Then the new set of poles is determined by the equation

$$1 + s\delta - \Phi' - \left(\frac{f_1 c_1}{s - \lambda_1} + \frac{f_1^* c_1^*}{s - \lambda_1^*} \right) s = 0.$$

We further take $|f_1 c_1|$ small, and correspondingly we write an expansion for the solution $s_n \approx s_n^{(0)} + \varepsilon s_n^{(1)}$, where ε is order $|f_1 c_1|$. At order zero, $s_n^{(0)}$ is one of the solutions of a third degree equation. These include one real solution, close to the s_0 transmission pole in Eq. (2.25). The first-order equation is first degree in $s_n^{(1)}$, such that we have three solutions $s_0^{(1)}$, $s_1^{(1)}$, and $s_{-1}^{(1)}$, one for each of the solutions at order zero. The complex solutions are

$$s_1 = \lambda_1 \left(1 + \frac{f_1 c_1}{1 - \Phi' + \lambda_1 \delta} \right), \quad (2.27)$$

and $s_{-1} = s_1^*$.

For the excitatory population ($\Phi' > 0$), Eq. (2.27) suggests that when $\Phi' \rightarrow 1$, and then when $|f_1 c_1|$ increases, $\tau_1 \equiv -1/\text{Re}(s_1)$, the longest characteristic time of the system, becomes small, so that the system reaches more quickly the steady state, as will be shown in Sec. III for a specific case.

Remembering that $\Phi = \Phi(\mu, \sigma^2)$, and taking into account that for an excitatory population both μ and σ^2 are monotonically increasing functions of the synaptic couplings (see, for instance, [33]), it is seen that an increase in the recurrent couplings brings about an increase in Φ' . This implies that if *learning* is expressed as a potentiation of the synaptic efficacies, this would be observed in the response time of the population to an external stimulation, so that a strengthened recurrent coupling can prime the population to respond quickly. We further discuss this point in Sec. III D, in the context of a specific model. Experimental evidence provides

some support for this statement (see, for example, Ref. [34]), which we feel would deserve further experimental investigation.

In the regions not too close to the stability boundary, s_1 (and the analogous poles s_n near λ_n) have real parts smaller in module than those of transmission poles, so that they are, in the situations of interest, responsible for the characteristic time of the approach to an asynchronous state ν_0 .

Turning to the imaginary part of s_1 , for the relatively low frequencies of collective oscillations represented by this pole (directly related to the eigenvalue λ_1), the remarks at the end of Sec. II C 1 apply. Since the above poles are intimately related to the pure “free” diffusion process, we term them *diffusion* poles.

In the low noise limit, the diffusion poles can be associated with the characteristic times and resonant frequencies observed in previous works using a mean-field approach with a deterministic afferent current [2,5,6,10], and called in [5] the *fine structure* of the spectrum. The variance of the recurrent afferent current, taken into account in the present theory, dramatically affects the behavior of the system (particularly in noise-dominated regimes), as was recognized in Refs. [6] and [22] for the case of external activity-independent noise.

The above resonant response due to the diffusion poles is never enough to challenge the network local stability; on the other hand, we discussed in the previous subsection that for suitable (large) delays, a “coupling” between the transmission and the diffusion poles emerges which facilitates the ignition of an unstable regime (driven anyway by the transmission poles) at frequencies around multiples of ν_0 .

3. Some remarks on the nature of the poles

To summarize the phenomenological implications of the above analysis, we list some remarks on the role and behavior of the two families of poles of $\nu_1(s)$ discussed in the previous subsections.

The diffusion poles (hereafter called $s_n^{(d)}$) do not affect the stability of the excitatory neural population [which is entirely due to the transmission poles ($s_n^{(t)}$)] since their real part is always negative, as that of the eigenvalues λ_n . Indeed we argued that for increasing Φ' , the $s_n^{(d)}$ get farther and farther from the imaginary axis, while the opposite is true for $s_n^{(t)}$, ultimately bringing the network to instability.

In many cases of interest (and perhaps in general), the real part of λ_n increases with increasing n , so that the relaxation times of the system are essentially determined by $s_1^{(d)}$. Thus, even if in principle we could have repeated the approximate calculation leading to Eq. (2.27) for any eigenvalue, that term is likely to provide the main contribution.

The transmission poles $s_n^{(t)}$ are analogous to those observed in Refs. [5] and [9], and disappear for a noninteracting network, or vanishing transmission delays. The diffusion poles $s_n^{(d)}$ are inherently related to the nature of the diffusion process describing the network’s dynamics in the mean-field approximation. They affect the network dynamics even in the noninteracting case, both governing the transient response of the network to a change in its inputs, and contributing low-

frequency components to the spectrum of the global activity for a *finite* network, as we show in the following section [35].

F. Finite-size effects

Finite N brings about both “incoherent” fluctuations, which are already taken care of in the mean-field theory, and “coherent” fluctuations, which give rise to new phenomena.

As for the first, in the presence of sparse connectivity (such that neurons share a negligible portion of common input), or other sources of quenched randomness affecting the interaction among neurons (effectively decorrelating neurons’ firings even for high connectivity), the stochastic changes of the current are sensed by different neurons as incoherent fluctuations [36]. These fluctuations are taken care of in the mean-field approach through $\sigma^2(v, t)$.

On the other hand, the number of spikes emitted in a time interval dt by the network is a Poisson variable with mean and variance $N\nu(t)dt$, as observed in Refs. [9,10]. The estimate of $\nu(t)$ [similarly to $p(v, t)$] is then a stochastic process $\nu_N(t)$, well described in the limit of large $N\nu$ by

$$\nu_N(t) = \nu(t) + \sqrt{\frac{\nu(t)}{N}}\Gamma(t), \quad (2.28)$$

where $\Gamma(t)$ is a white noise as in the Langevin equation (2.1), and $\nu(t)$ is the probability of emitting a spike per unit time in the infinite network. Such finite- N fluctuations, which affect the global activity ν_N , are coherently felt by all neurons in the network: The now stochastic moments $\mu(v, \nu_N(t))$ and $\sigma^2(v, \nu_N(t))$ of the afferent current all experience the same fluctuation, since they are driven by the collective activity ν_N . This approach leads then to a “stochastic version” of the Fokker-Planck operator L , L_N , and consequently of Eq. (2.3). Stochasticity disappears in the limit $N \rightarrow \infty$ because

$$\lim_{N \rightarrow \infty} \nu_N(t) = \nu(t).$$

Besides affecting μ and σ^2 , further finite- N effects are related to fluctuations at θ and H . The flux $\nu_N(t)$ exiting θ reenters at the reset potential H , determining a departure from the boundary condition (2.7), due to a stochastic source of realizations, not present in the infinite- N limit. The net flux conservation can be recovered by adding a multiplicative noise to the Fokker-Planck equation, representing the stochastic fluctuation of the reentering flux, with respect to its expected value in the infinite- N limit:

$$\begin{aligned} \partial_t p(v, t) &= L_N p(v, t) + \delta(v - H)[\nu_N(t) - \nu(t)] \\ &= L_N p(v, t) + \delta(v - H) \sqrt{\frac{\nu(t)}{N}}\Gamma(t). \end{aligned} \quad (2.29)$$

This equation, together with Eq. (2.28), describes the dynamics of a population of neurons for finite N , and we can now try to derive the finite- N emission rate equation analogous to Eq. (2.18).

Before that, a remark is in order: The above description in terms of $\nu(t)$ and $p(v, t)$, which are the infinite- N dynamic variables, is justified in this context because in this context the neurons interact only through the emitted spikes: Two different membrane potentials $V_i(t)$ and $V_j(t)$ do not directly interact. The interplay between the two levels of description (ν_N, p_N) and (ν, p) can be viewed as follows: For finite N , each V still evolves, as already remarked, according to the Langevin equation (2.1), since to a very good approximation its afferent current is a δ -correlated Gaussian process; so, the purely diffusive part of the collective dynamics is still captured by the Fokker-Planck equation for p , the evolution equation for an infinite ensemble of neurons. Then, we have to take the finite N into account on the boundaries (i.e., upon spikes emission), which in a sense make a finite subset of the infinite number of neurons “real.”

As a complete set over which to expand the above stochastic Fokker-Planck equation, we still take the eigenfunctions of L_N with their eigenvalues, which are now stochastic, explicit functions of ν_N . The use of this stochastic moving basis leads to the following expression for the emission rate equation:

$$\begin{aligned} \dot{\vec{a}} &= (\mathbf{\Lambda} + \mathbf{C}\dot{\nu}_N)\vec{a} + \vec{c}\dot{\nu}_N + \vec{\psi}\sqrt{\nu/N}\Gamma, \\ \nu &= \Phi + \vec{f} \cdot \vec{a}, \\ \nu_N &= \nu + \sqrt{\nu/N}\Gamma, \end{aligned} \quad (2.30)$$

where the elements of $\vec{\psi}$ are the nonstationary eigenfunctions of the adjoint operator L_N^+ , evaluated at the reset potential, $\psi_n(H, t)$. For simplicity, we omitted the dependence on time, which is the same as in Eq. (2.21). It should be noted that the above stochastic emission rate equation exhibits a complicated dependence on the finite-size noise, with $\mathbf{\Lambda}$, \mathbf{C} , and \vec{c} all functions of ν_N : This is the expression of the noisy nature of the operator L_N in this context.

The above fluctuations act as an ongoing series of instantaneous endogenous perturbations, and as such they probe the characteristic times of the system. This will show up very clearly in the study of the finite- N power spectral density of the collective activity, as we will see later.

From Eq. (2.30), we see how the two sources of stochasticity (the fluctuations of the moments of the afferent current, leading to L_N , and those of the reentering flux into the reset potential H) make the dynamics of the coefficients $a_n(t)$ [and therefore the nature of $p(v, t)$] stochastic.

In order to single out the different sources of noise, it is useful to discuss again the case of noninteracting neurons, when the moments of the afferent current are independent of the emission rate ν of the neuron population, the Fokker-Planck operator L is deterministic as its eigenvalues and eigenfunctions, and the coupling terms vanish, so that the emission rate equation reduces to

$$\begin{aligned} \dot{\vec{a}} &= \mathbf{\Lambda}\vec{a} + \vec{\psi}\sqrt{\nu/N}\Gamma, \\ \nu &= \Phi + \vec{f} \cdot \vec{a}, \end{aligned}$$

$$\nu_N = \nu + \sqrt{\nu/N}\Gamma.$$

For drift-dominated regimes, all the a_n are complex stochastic processes driven by the same δ -correlated noise, and we can prove that each one of them has to a good approximation a resonant frequency in $\text{Im}\lambda_n \simeq n\nu$. Since ν_N is a linear function of a through ν , the spectral content of a will endow ν_N with nontrivial spectral properties. We emphasize that this happens for a noninteracting network, and it is a manifestation of the finite- N fluctuations not included in those of μ and σ^2 .

Intuitively, for drift-dominated regimes, a large fluctuation in p , due to the reentering flux in H , propagates essentially undeformed towards θ , since in that regime it is not spread much by the diffusion.

1. Local analysis

Asynchronous states are now represented by a distribution of emission rates around the mean-field fixed point ν_0 . The local analysis described in the previous section can be applied in the same way to this case. We assume the zero-order contribution to be deterministic and constant, and the stochastic component only affect the first and higher orders of perturbations, so that for large enough N , the leading contribution of the stochastic driving force $\sqrt{\nu(t)/N}\Gamma(t) = \sqrt{[\nu_0 + \nu_1(t) + \dots]}/N\Gamma(t)$ is

$$\eta_0(t) = \sqrt{\frac{\nu_0}{N}}\Gamma(t)$$

and we will then write

$$\begin{aligned} \dot{\vec{a}}_1(t) &= \Lambda\vec{a}_1(t) + \vec{c}\dot{\nu}_1(t - \delta) + \vec{\psi}\eta_0(t), \\ \nu_1(t) &= \Phi'\nu_1(t - \delta) + \vec{f}\cdot\vec{a}_1(t) + \eta_0(t), \end{aligned} \quad (2.31)$$

where all the time-independent terms are evaluated at $\nu(t) = \nu_0$.

The previously discussed questions about the stability and the transients are not altered by the finite-size effects, as the pole composition of the Laplace transform $\nu_1(s)$ of $\nu_1(t)$ is unaffected by the presence of η_0 , which enters the numerator.

2. Power spectral density

Under the conditions of validity of the local analysis, the system is stochastic and linear, and can be fully characterized by the driving white noise $\eta_0(t)$, whose power spectrum $|\eta_0(\omega)|^2$ is ν_0/N , and the transfer function (the Fourier transform of the impulsive response), $T_1(\omega)$,

$$T_1(\omega) = \frac{1 + \vec{f}\cdot(i\omega\mathbf{I} - \Lambda)^{-1}\vec{\psi}}{(1 - \Phi'e^{-i\omega\delta}) - i\vec{f}\cdot(i\omega\mathbf{I} - \Lambda)^{-1}\vec{c}\omega e^{-i\omega\delta}}.$$

If one wants to consider the contribution of the average ν_0 to the emission rate $\nu(t)$, a term proportional to $\delta(\omega)$ has to be added, which we omit for simplicity.

The power spectrum $P_1(\omega)$ of $\nu_1(t)$ is then given by

$$\begin{aligned} P_1(\omega) &= |T_1(\omega)\eta_0(\omega)|^2 \\ &= \frac{|1 + \vec{f}\cdot(i\omega\mathbf{I} - \Lambda)^{-1}\vec{\psi}|^2}{|(e^{i\omega\delta} - \Phi') - i\vec{f}\cdot(i\omega\mathbf{I} - \Lambda)^{-1}\vec{c}\omega|^2} \frac{\nu_0}{N}. \end{aligned} \quad (2.32)$$

$P_1(\omega)$ has two series of peaks: one is centered around the imaginary part of the poles s_n (the resonant frequencies of the system), whose width is proportional to $\text{Re}s_n$. As we will see in the next section, this provides evidence that in a system of coupled spiking neurons, macroscopically different characteristic times coexist (as suggested by experimental evidence in the study of the cross-correlation function of neuron activity). They span a range from very low (~ 10 Hz) to high frequency of the order of $1/\delta$; these latter peaks have been recognized in [5,9].

The numerator modulates the spectrum, inducing a second set of peaks corresponding to the λ . So we can recognize two qualitatively different finite- N contributions to $P_1(\omega)$: one is related to going from L to L_N in Eq. (2.29) and produces the first set of peaks; it has in principle a global effect on $P_1(\omega)$, but it turns out to significantly affect only the high- ω part related to transmission poles. The other finite- N contribution to $P_1(\omega)$ is the one determined by the fluctuations of the reentering flux at H , and has a major effect for low ω (at least for drift-dominated regimes). This provides phenomenological evidence for the role of the latter source of finite- N noise.

The numerator of Eq. (2.32) is the only element that does not vanish when the neurons are uncoupled ($\Phi' = 0$ and $\vec{c} = 0$),

$$P_1(\omega) = |1 + \vec{f}\cdot(i\omega\mathbf{I} - \Lambda)^{-1}\vec{\psi}|^2 \frac{\nu_0}{N}. \quad (2.33)$$

It provides a nontrivial contribution only at low frequency, since

$$\vec{f}\cdot(i\omega\mathbf{I} - \Lambda)^{-1}\vec{\psi} = \sum_{n \neq 0} \frac{f_n \psi_n(H)}{i\omega - \lambda_n}$$

tends to zero when $\omega \rightarrow \infty$, where $P_1(\omega)$ approaches the power spectrum of a white noise. At low frequency we expect to see some resonant peaks around $\text{Im}\lambda_n$, at least in strongly drift-dominated (suprathreshold) regimes (remember that we conjecture and verify later in a specific case that $\text{Im}\lambda_n = 0$ for noise-dominated regimes).

This component of the power spectrum originates from the diffusive transport of the fluctuations of $p(v, t)$ induced at the reset potential by the reentering stochastic flux. Its contribution is not negligible only for those regimes that allow a slow forgetting of the history of the depolarization, as it is the case for drift-dominated regimes.

If a distribution of delays is introduced, it can be argued (and partially verified in simulations) that the high- ω part of the spectrum gets flattened, thus affecting mostly the transmission part of the spectrum. This, we expect, has implications for the stability of the network, since the damping of

the high-frequency tail of the spectrum can be viewed as an effective increase of the real part of the high- ω transmission poles, thereby helping keeping the system away from the stability boundary (see also Ref. [9] for a similar remark).

G. Several interacting populations

The approach discussed in the previous subsections has a straightforward extension to the case of several interacting populations of IF neurons. Following a common practice in the mean-field analysis, the network of interacting neurons is partitioned in ‘‘homogeneous populations,’’ each composed of a subset of neurons which are structurally identical (same emission threshold, same leakage term, etc.) and share the same statistical properties of their afferent current (i.e., μ and σ^2), emitting then spikes at the same rate. This partitioning accounts for structurally different (e.g., excitatory versus inhibitory) or functionally different (e.g., stimulated versus nonstimulated) neurons. In this case, for each population α there is a Fokker-Planck equation with its operator L_α , depending on the moments μ_α and σ_α^2 of the afferent current, probability density function $p_\alpha(v, t)$, and emission rate ν_α . All of these variables are now functions of the activity of all the (say) P populations, so that $\mu_\alpha = \mu_\alpha(\vec{\nu})$ and $\sigma_\alpha^2 = \sigma_\alpha^2(\vec{\nu})$, where $\vec{\nu} = \{\nu_\alpha\}_1^P$.

The (infinite- N) emission rate equation becomes

$$\dot{\vec{a}}_\alpha = \left(\Lambda_\alpha + \sum_{\beta=1}^P \mathbf{C}_{\alpha\beta} \dot{\nu}_\beta \right) \vec{a}_\alpha + \sum_{\beta=1}^P \vec{c}_{\alpha\beta} \dot{\nu}_\beta,$$

$$\nu_\alpha = \Phi_\alpha + \vec{f}_\alpha \cdot \vec{a}_\alpha$$

for any $\alpha \in [1, P]$, where \vec{a}_α is the vector of the modal expansion coefficients of the p.d.f. p_α , the flux vector is $\vec{f}_\alpha = \vec{f}_\alpha(\mu_\alpha, \sigma_\alpha^2)$, the population gain function is $\Phi_\alpha = \Phi_\alpha(\mu_\alpha, \sigma_\alpha^2)$, the diagonal matrix of the eigenvalues is $\Lambda_\alpha = \Lambda_\alpha(\mu_\alpha, \sigma_\alpha^2)$, and the coupling matrix \mathbf{C} and vector \vec{c} are now expressions not only of the recurrent interaction (α, α) but also of the coupling between different populations (α, β),

$$\vec{c}_{\alpha\beta} = \{ \langle \partial_{\nu_\beta} \psi_{an}(\mu_\alpha, \sigma_\alpha^2) | \phi_{\alpha 0}(\mu_\alpha, \sigma_\alpha^2) \rangle \}_{n \neq 0}$$

and

$$\mathbf{C}_{\alpha\beta} = \{ \langle \partial_{\nu_\beta} \psi_{an}(\mu_\alpha, \sigma_\alpha^2) | \phi_{\alpha m}(\mu_\alpha, \sigma_\alpha^2) \rangle \}_{n \neq 0}.$$

It should be noted that if neurons belonging to different populations differ only for the afferent current, taking into account several interacting populations does not require us to study anew the Fokker-Planck operator L and its eigenvalues and eigenfunctions, so that the above expansion relies upon the same information needed for the case of a single population. This is due to the particular functional dependence on the activity of the different populations, which is always ‘‘seen’’ through the moments μ_α and σ_α^2 of the afferent currents.

By such an extension, the present formalism can embody the study of multipopulation systems of IF neurons, performed under various viewpoints and with different tools by many authors [5,8,37,13,38] (see also [39,40]).

It can be interesting to observe that such an approach allows us in principle, in the limit of an infinite number of populations, to study the case of an inhomogeneous population, viewed as a collection of small (but large enough to satisfy the mean-field hypotheses) interacting homogeneous populations (as discussed in Refs. [5,7]). The case of spatially structured networks of neurons can then be approached along these lines, and it is part of planned future work.

III. AN EXAMPLE: ONE POPULATION OF LINEAR IF NEURONS

Because of its amenability to analytical treatment, we specialize the above analysis to the linear IF neuron (LIF) [12], whose depolarization is described by a Wiener process with drift, having a reflecting barrier at $v_{\min}=0$, which we also choose as the reset potential ($H=0$). It was proven in [12,31] that networks of IF neurons retain most of the collective properties of those composed of leaky IF neurons. The decay term is constant: $f(v) = -\beta$. For simplicity here we set $\mu(t) - \beta \rightarrow \mu(t)$, considering β as a constant inhibitory afferent current, and the corresponding Fokker-Planck operator L_{LIF} becomes

$$L_{\text{LIF}}(v, t) = -\mu(t) \partial_v + \frac{1}{2} \sigma^2(t) \partial_v^2.$$

Equation (2.9) is therefore a homogeneous second-order differential equation with constant coefficients, whose general solution, if $\lambda \neq 0$, is

$$\phi_\lambda(v, t) = [c_+ e^{\xi v / \theta} + c_- e^{-\xi v / \theta}] e^{\frac{\xi v}{\theta}} \quad (3.1)$$

(valid for $\zeta \neq 0$), where we set

$$\zeta(\lambda) \equiv \frac{\theta}{\sigma^2} \sqrt{\mu^2 + 2\sigma^2 \lambda},$$

$$\xi \equiv \frac{\mu \theta}{\sigma^2}. \quad (3.2)$$

The spectrum of the operator, and the arbitrary constants in its eigenfunctions, are determined by the boundary conditions, as we show in the following.

From Eq. (2.11), the adjoint operator for this specific model is

$$L_{\text{LIF}}^+(v, t) = \mu(t) \partial_v + \frac{1}{2} \sigma^2(t) \partial_v^2,$$

and its eigenfunctions ψ_λ are

$$\psi_\lambda(v, t) = [c_+ e^{\xi v / \theta} + c_- e^{-\xi v / \theta}] e^{-\xi v / \theta}.$$

A. Eigenvalues and eigenfunctions of L_{LIF}

1. The stationary mode: $\lambda=0$

$\lambda=0$ is an eigenvalue of L . The corresponding eigenfunction, which in general depends on time through μ and σ^2 , is

$$\phi_0(v,t) = \frac{c}{\mu} [1 - e^{-2\xi(\theta-v)/\theta}],$$

where c is given by the normalization condition

$$c \equiv \Phi(\mu, \sigma^2) = \left[\frac{\sigma^2}{2\mu^2} \left(\frac{2\mu\theta}{\sigma^2} - 1 + e^{-2\mu\theta/\sigma^2} \right) \right]^{-1},$$

the current-to-rate transduction function derived in Ref. [12]. In stationary condition $\Phi(\mu, \sigma^2)$ gives the output emission rate ν of the population (its gain function) and ϕ_0 is the p.d.f. $p(v)$ of the membrane potential at any time.

Recall that the eigenfunction ψ_0 of the adjoint operator L_{LIF}^+ is

$$\psi_0 = 1.$$

2. The nonstationary modes

To characterize the spectrum of the operator L_{LIF} , we study the generic eigenfunction $\phi_\lambda(v,t)$ for $\lambda \neq 0$ with the boundary conditions appropriate for the LIF neuron.

The presence of the absorbing barrier (2.5) constrains Eq. (3.1) to the form

$$\phi_\lambda(v,t) = c_\lambda e^{\xi v/\theta} \sinh \frac{\zeta(\theta-v)}{\theta}, \quad (3.3)$$

which, due to the flux conservation (2.7) and the reflecting barrier (2.8), satisfies the following equation:

$$\frac{1}{2} \sigma^2 \partial_v \phi_\lambda|_{v=\theta} = (\frac{1}{2} \sigma^2 \partial_v \phi_\lambda - \mu \phi_\lambda)|_{v \rightarrow 0^+}.$$

From this we find the *characteristic equation*

$$\zeta e^\xi = \zeta \cosh \zeta + \xi \sinh \zeta, \quad (3.4)$$

whose solutions give the set of all the nonvanishing eigenvalues of the operator L_{LIF} . It is easy to verify from these equations the property $\int \phi_\lambda(v,t) dv = 0$.

Before discussing the characteristic equation, we study the eigenfunctions of the adjoint operator L_{LIF}^+ , taking into account the corresponding boundary conditions: $\psi_\lambda(\theta) = \psi_\lambda(0)$ and $\partial_v \psi_\lambda(0) = 0$. We obtain again Eq. (3.4), consistently with the known property that the eigenvalues are the same as those of L_{LIF} , and the following expression for the eigenfunctions:

$$\psi_\lambda(v,t) = e^{-\xi v/\theta} \left[\zeta \cosh \frac{\zeta v}{\theta} + \xi \sinh \frac{\zeta v}{\theta} \right]. \quad (3.5)$$

In the above equation, we omitted the integration constant, because we can absorb it in the c_λ of ϕ_λ . This constant c_λ in Eq. (3.3) is complex and can be determined from the biorthonormality condition (2.13), as in the case of the

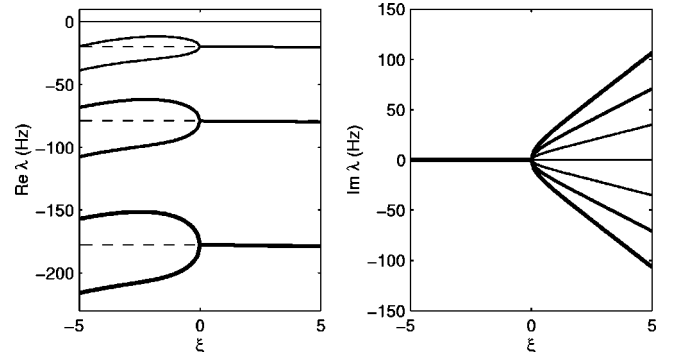


FIG. 1. The spectrum of L_{LIF} as a function of ξ . Real (left) and imaginary (right) parts of the eigenvalues of L_{LIF} λ_n ($n \in [-3,3]$), for ξ varying in the same interval. In the $\text{Re } \lambda(\xi)$ plot the dashed lines are the reference values $-2\pi^2 n^2$, for $\xi=0$. We set for simplicity $\sigma^2=1$ and $\theta=1$. See text for details.

stationary mode. Making use of the characteristic equation, it is not hard to prove that $\langle \psi_{\lambda'} | \phi_\lambda \rangle = 0$ when $\lambda' \neq \lambda$, whereas the normalization condition $\langle \psi_\lambda | \phi_\lambda \rangle = 1$ requires

$$c_\lambda = \frac{2\zeta}{\theta [\zeta \xi \cosh \zeta + (\zeta^2 - \xi) \sinh \zeta]}.$$

3. The spectrum of L_{LIF}

For the sake of brevity, we do not give the details of the computation of the eigenvalues of L_{LIF} , and we just summarize below the key features of the result (details of the computation are available from the authors upon request).

Figure 1 shows the first seven eigenvalues (including $\lambda=0$) as a function of ξ . First of all, we note that $\text{Re } \lambda \leq 0$, as expected. It is also apparent that the real and imaginary parts of λ have an abrupt transition when the input current goes from a noise-dominated regime ($\xi < 0$, i.e., negative total drift) to a drift-dominated one ($\xi > 0$, i.e., positive total drift): In the first case, the eigenvalues are real and negative, whereas if the drift is positive, the eigenvalues are complex.

To summarize, one eigenvalue of L_{LIF} is

$$\lambda_0 = 0$$

for any dynamic regime. The other eigenvalues are, for $\xi = 0$,

$$\lambda_n(0) = -\frac{\sigma^2}{\theta^2} 2\pi^2 n^2$$

for any integer $n \neq 0$.

It turns out that $\text{Re } \lambda_n(\xi) \sim -2\pi^2 n^2 \sigma^2 / \theta^2 - O(\xi)$, which suggests that the characteristic times associated with eigenvalues λ_n decrease like $1/n^2$ when n increases, leading us to assume that in a quasistationary regime only the first eigenvalues play an important role: The modes are exponentially damped with characteristic times $|\text{Re } \lambda_n|^{-1} \sim 1/(n\sigma)^2$ (see also Sec. II E 3). This also suggests that the noise in the afferent current plays an important role for uncoupled net-

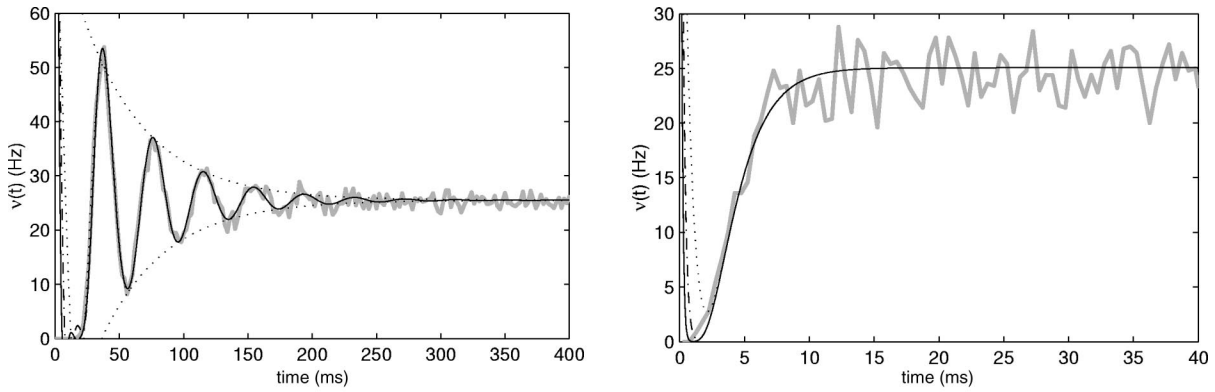


FIG. 2. Transient response of a population of uncoupled neurons: Simulations vs theory. The initial condition is $V(0)=0$ for all the neurons. At $t=0$ a current is injected, with the same constant μ and σ^2 for all the neurons, such as to asymptotically drive the neurons to fire at $\nu_0=25$ Hz. The upper and lower plots refer to neurons in drift-dominated and noise-dominated regimes, respectively. Light gray lines are the emission rate of 10 000 simulated IF neurons; dashed-dotted, dashed, and solid lines are the theoretical emission rates due to the first, second, and third (couples of) modes, respectively. Damped oscillations are visible only in the drift-dominated regime, mainly due to the first eigenvalue of L (dotted lines are the real parts of the first modes).

works: The greater the fluctuations in the afferent current, the shorter the response time, as expected.

As we will see in the following section, in the absence of interaction between neurons, the imaginary part of the eigenvalues, which appears only in a drift-dominated regime, accounts for the oscillatory behavior of the population emission rate. Such oscillation is dominated by the first spectral term ($n=1$), and its period is given by $2\pi/|\text{Im}\lambda_1| \approx \theta/\mu \approx 1/\nu$, which is the time a neuron takes, in the absence of noise, to reach the threshold starting from $V=0$.

B. A first check: Noninteracting neurons

For an ensemble of noninteracting neurons, $\nu(t)$ is given by Eq. (2.20), where the fluxes f_n , defined by Eq. (2.19), are evaluated using eigenstates ϕ_n given by Eq. (3.3). If we further assume the initial condition $p(v, t=0) = \delta(v)$, the result is

$$\nu(t) = \Phi(\mu, \sigma^2) + \frac{\sigma^2}{2\theta} e^{\xi} \sum_{n \neq 0} c(\lambda_n) \zeta(\lambda_n)^2 e^{\lambda_n t}.$$

Theoretical predictions, and the range of validity of the approximations involved, are checked against simulations (and also numerical integration, not shown) of the Fokker-Planck equation.

Figure 2 shows the population emission rate versus time, for an ensemble of uncoupled LIF neurons, in a drift-dominated (top) and in a noise-dominated (bottom) regime.

Neurons all start integrating the afferent current from the initial condition $V=0$, and parameters are such as to have a stable, 25 Hz firing rate as a fixed point. The figure is meant to illustrate how drift- or noise-dominated regimes imply very different transient responses: damped oscillatory in the former case and exponentially approaching the asymptotic state for the latter, as predicted by the theory. The quantitative agreement between theory (solid black line) and simulation (gray line, average activity of 10 000 simulated LIF neurons) is remarkable. We note that only six spectral terms (the

first three eigenmodes and their complex conjugates) are enough to account for the properties of the transient response with high accuracy; furthermore, in the cases shown, the hierarchy of characteristic times is such that after a few milliseconds the first eigenvalue alone guides the evolution of ν (the real part of the first term is the dotted line in the plots). The very early stages are not well reproduced, since more and more terms would be needed as we go towards $t=0$; a modest improvement over the first mode due to the inclusion of the next two is barely visible in the second plot. The hierarchy of times pertaining to the successive eigenvalues is clearly illustrated in Fig. 1.

We remark that the numerical integration of the Fokker-Planck equation (not shown) is in excellent agreement with the simulation, which proves that the hypotheses underlying the theory are fulfilled.

The spectral properties associated with the stationary state are illustrated in Fig. 3. We recall that a nontrivial spectral structure (modulating the constant, white noise ν_0/N spectrum) appears as a result of finite-size effects on the probability current at the boundaries, and, since we are dealing with uncoupled neurons, the transmission poles do not contribute. The figure shows a comparison between the theoretically predicted spectrum, Eq. (2.33), and the one derived from simulations. The position of the peaks is determined by the imaginary part of the diffusion poles (which coincide with the eigenvalues for the uncoupled network). The real part of the poles determines the height and width of the peaks. Similar results have been found in Ref. [10], and also in Refs. [2,15].

C. Populations of interacting neurons

1. A network of inhibitory neurons

We now move to the more interesting case of a population of interacting neurons, and test the theoretical predictions concerning the transient behavior and the spectral properties. We first show in Fig. 4 the distribution of the poles of $\nu_1(s)$ [Eq. (2.23)] for a population of interacting inhibitory neu-

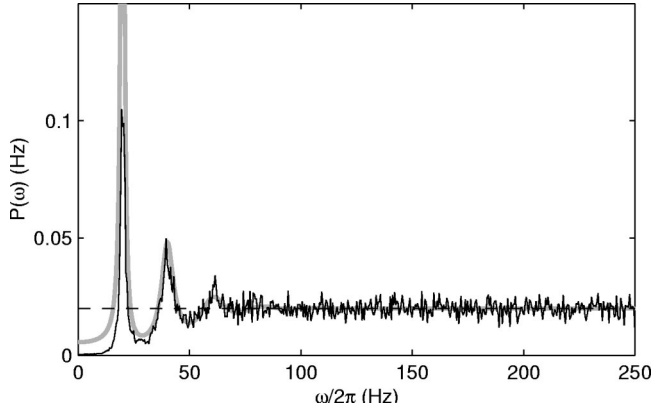


FIG. 3. Power spectrum of the activity of a population of uncoupled neurons in a drift-dominated regime: Simulations vs theory. The solid line is the power spectrum from a simulation of 60 sec in a stationary condition (after decay of the transient); the thick gray line is the theoretical prediction; the dashed line is the flat power spectrum of the white noise with variance ν_0/N ($\nu_0=20$ Hz and $N=1000$).

rons. The diffusion and transmission poles are plotted in the complex plane for 13 values of Φ' , all corresponding to the same fixed-point emission rate (by adjusting external currents and couplings).

It is seen that for the diffusion poles, the real part stays negative, while that of the transmission poles ultimately crosses the imaginary axis for high enough coupling, thereby determining the instability of the fixed point. It is also apparent from the plot that the imaginary part of both the transmission and the diffusion poles (the frequency of the associated oscillations) is essentially constant with respect to Φ' , while the characteristic times of the transient response, associated with the real part, are very sensitive to Φ' , and therefore to the coupling (stronger coupling, quicker response). For inhibitory neurons, the transmission poles always have a nonvanishing imaginary part; this suggests the oscillatory nature of the instability, when the real part of $s^{(t)}$ becomes positive. In fact, it was proved in [9] (see also Ref. [31]) that the inhibitory network undergoes a Hopf bifurcation. Up to tiny variations, for all the shown values of Φ' , $\text{Im } s_n^{(t)} = \pi(2n-1)/\delta$.

Figure 5 shows the distribution of the diffusion and transmission poles in the complex plane for an inhibitory population in a noise-dominated regime. Markers and shading are as in Fig. 4. The network is stable for all the points shown (though it is still true that the transmission poles are responsible for the instability of the network for high enough couplings). It is seen that in this case the real part of the diffusion poles has a weak dependence on the couplings, while the associated imaginary parts strongly depend on them. We also stress that the diffusion poles exhibit an imaginary part, even if the eigenvalues of L are real.

Figures 6, 7, and 8 compare, for coupled inhibitory networks, theoretical predictions to simulations (details are in the captions). We remark that, as anticipated, finite-size fluctuations do not affect the transient behavior of the network, and Fig. 6 illustrates the excellent agreement between simu-

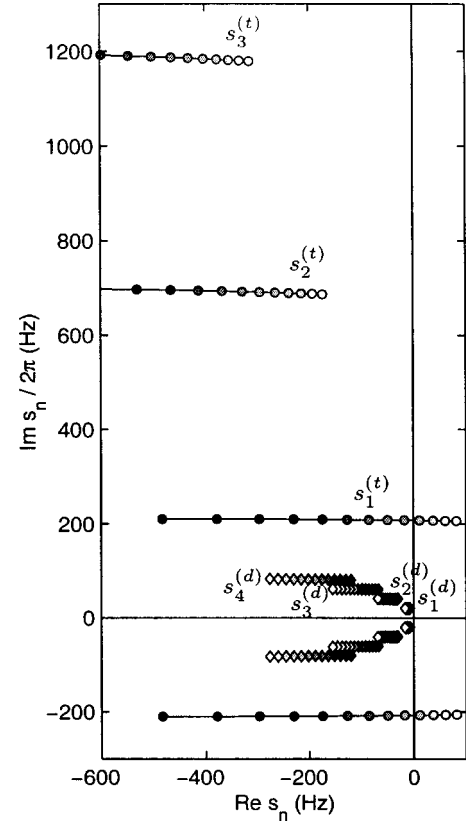


FIG. 4. Poles distribution for a recurrent inhibitory population with different coupling strengths in a drift-dominated regime. Diamonds: first four diffusion poles ($s_n^{(d)}$); circles: first three transmission poles ($s_n^{(t)}$) (poles are complex-conjugate pairs). The darker the marker, the smaller (in module) the slope of the transfer function and the coupling strength. $s_1^{(t)}$ (with its complex conjugate) is the first pole crossing the imaginary axes, determining the instability of the population dynamics. For different coupling strengths the external currents are adjusted in order to have the same fixed point at $\nu_0=20$ Hz. It is clearly seen in the figure that the diffusion and the transmission poles move in opposite directions along the real axis, when Φ' is varied.

lations and the theoretical predictions in the infinite volume limit.

Figure 7 shows the power spectral density of the population activity, theory versus simulation. The population activity has been sampled from simulation after the transient was extinguished, in order to capture only the stationary spectrum. Besides the apparent good agreement between theory and simulations, we note the following: (i) the position of the high-frequency (transmission) peaks is unaffected by finite-size effects, coherently with the stated irrelevance of the latter for the poles of ν_1 (see remarks at the end of Sec. II F 1) (compare the position of the peaks with the imaginary parts of $s_n^{(t)}$ in Fig. 4); (ii) even if also the frequencies of the peaks potentially due to the diffusion poles are insensitive to finite- N fluctuations, the low- ω part of the spectrum is strongly affected: new peaks appear, at frequencies determined by the imaginary part of the eigenvalues of L , as a result of the ψ -dependent term in Eq. (2.32), which captures the effects of the fluctuations of the reentering flux in H ; the latter, finite- N

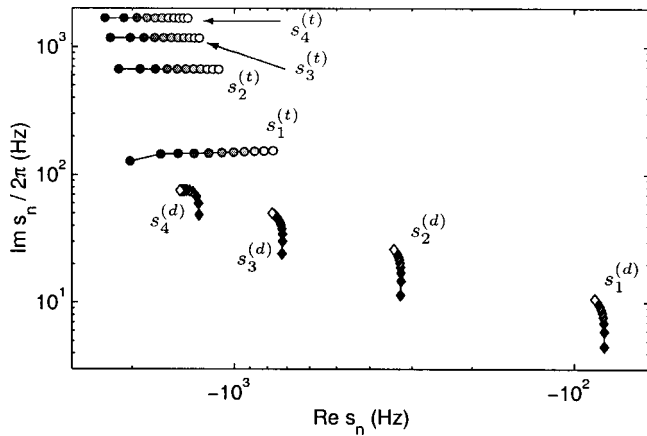


FIG. 5. Poles distribution for a recurrent inhibitory population with different coupling strengths in noise-dominated regimes. Diamonds: first four diffusion poles ($s_n^{(d)}$); circles: first four transmission poles ($s_n^{(t)}$). Shading as in Fig. 4. The mean population emission rate is kept at $\nu_0=4$ Hz. All the states are stable. Diffusion poles have a large spread in their imaginary parts, while the real parts of the two classes of poles still move in opposite directions, when Φ' is varied. Despite the fact that the eigenvalues of L are real in noise-dominated regimes, the diffusion poles are complex conjugates.

low-frequency part of the spectrum disappears for a population in a noise-dominated regime, since in this case the eigenvalues of L are purely real (see the discussion in Sec. IIF2).

We emphasize that the low- ω peaks in $P(\omega)$ are a qualitatively different consequence of the finite- N effects, with respect to the ω -independent term ν_0/N , which simply renormalizes the scale of $P(\omega)$, and would result from Pois-

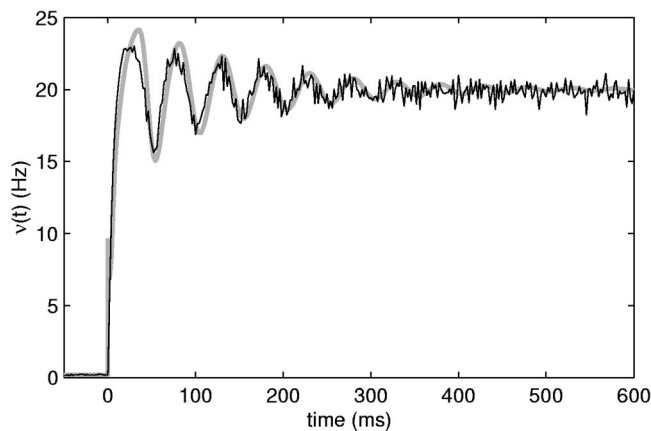


FIG. 6. Transient response to a step change in the external emission rate of a population of inhibitory neurons in a drift-dominated regime: Simulations vs theory. For $t < 0$, the network is in an asynchronous stationary state with mean emission rate $\nu=0.2$ Hz. At $t=0$, an instantaneous increase of the rate of external neurons, thereafter kept constant, drives the activity towards a new stable state with $\nu=20$ Hz. The solid black line is the mean of the activity from 10 simulations of a coupled network (5000 inhibitory LIF neurons). The thick gray line is the theoretical prediction, obtained from the first four pairs of diffusion poles.

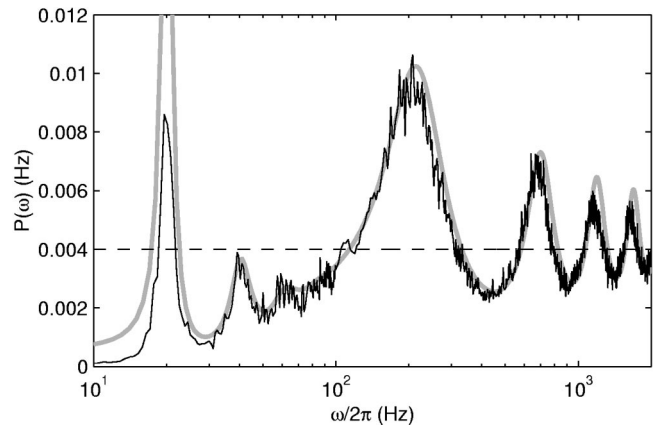


FIG. 7. Power spectrum of the activity of a population of inhibitory neurons in a stationary, drift-dominated regime: Simulations vs theory. The solid black line is the power spectrum from a 60-sec simulation; the thick gray line is the theoretical prediction; the dashed line is the power spectrum of the white noise with variance ν_0/N , being $\nu_0=20$ Hz and $N=5000$.

son fluctuations of μ , as introduced in [9]. The new finite- N , ω -dependent part of the spectrum can overwhelm the purely diffusive part (this is the case for the network in Fig. 7). We further note that this low- ω part of the spectrum becomes increasingly relevant if a distribution of delays is introduced; in fact, we checked (but do not show) that the high-frequency part of $P(\omega)$ is more and more strongly damped as the distribution of delays becomes wider (see Sec. IIF2).

Figure 8 shows the power spectrum of the collective activity for an inhibitory population in a noise-dominated regime. The eigenvalues of L are in this case purely real, and the power spectrum does not exhibit low-frequency peaks, even if in principle one could have expected them, in connection with the diffusion poles shown in Fig. 5; this means that, at least in this case, the numerator only of Eq. (2.32) determines the low- ω peaks in the spectrum.

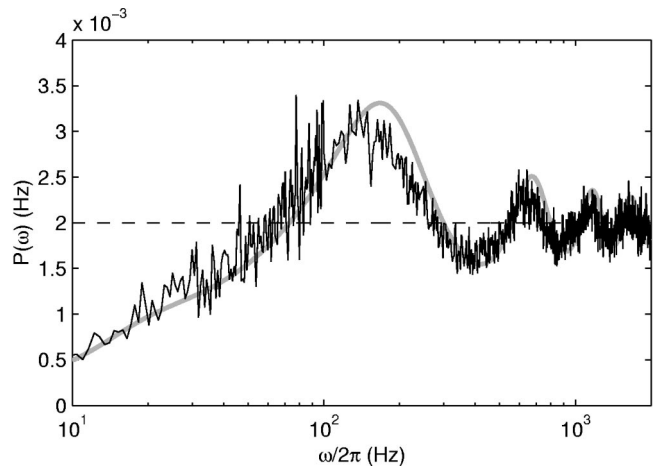


FIG. 8. Power spectrum of the activity of a population of inhibitory neurons in a stationary, noise-dominated regime: Simulations vs theory. The network parameters are the same as those of the white markers in Fig. 5. See Fig. 7 for details; in this case $\nu_0=4$ Hz and $N=2000$.

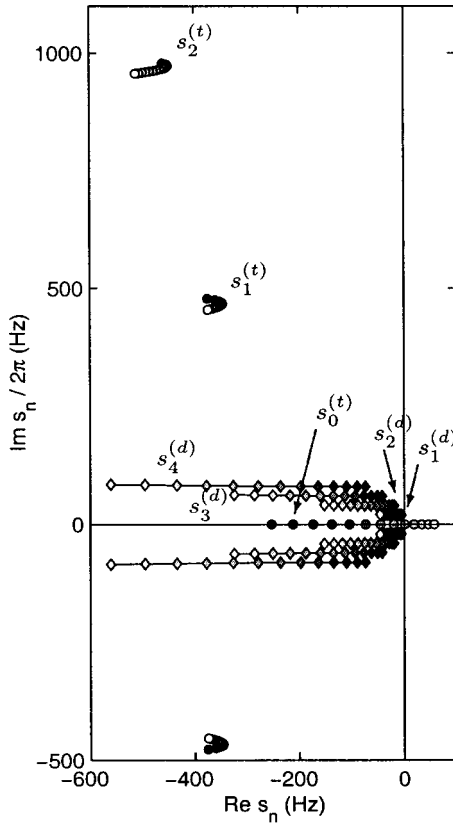


FIG. 9. Poles distribution for a recurrent excitatory population, for different coupling strengths in drift-dominated regimes. Diamonds: The first four diffusion poles ($s_n^{(d)}$); circles: The first three transmission poles ($s_n^{(t)}$) (poles are complex-conjugate pairs with the exception of $s_0^{(t)}$, which is real). See text and Fig. 4 for details. The transmission poles are shifted by a frequency $\sim 1/2\delta$ ($\delta = 2$ ms) with respect to the case of an inhibitory population. For the different coupling strengths, the external current is adjusted in order to have the same stationary rate $\nu_0 = 20$ Hz.

Comparing Figs. 8 and 7, it is apparent that the low- ω part of the power spectrum of the simulated network is in excellent agreement with the theory in the case of the noise-dominated regime, while a discrepancy arises for the drift-dominated case (with respect to the width and height of the peaks, while the resonant frequencies are still in good agreement). The trough in $P(\omega)$ for low ω is reminiscent of the effect of a refractory period on the power spectrum of the single neurons (see [10,41]); even if we assumed $\tau_0 = 0$, this does not exclude an effective refractory period possibly related to the transport of $p(v)$ along the interval (H, θ) in the drift-dominated regime.

2. A network of excitatory neurons

Figures 9–11 illustrate the stability scenario, the characteristic times of the transient response, and the power spectral density for a population of interacting excitatory neurons. From Fig. 9, two main differences are apparent, with respect to the inhibitory case. (i) The ν_1 now has the first transmission pole on the real axis, which implies a different nature of the transition to instability, no longer of the Hopf

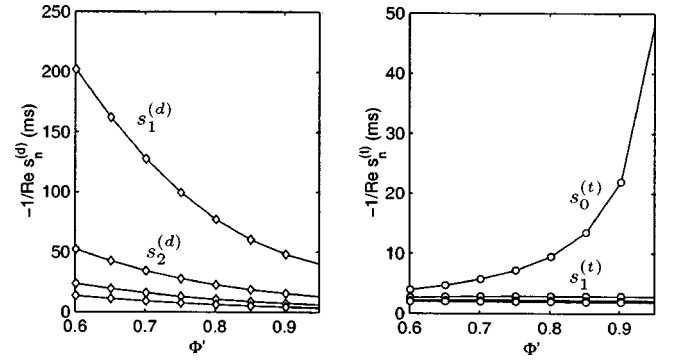


FIG. 10. Response times for a recurrent excitatory population with different coupling strengths. The response times of the first four diffusion poles (left) and four transmission poles (right) are plotted against Φ' . The two types of poles have a different behavior when the coupling strength (directly related to Φ') is increased: The response time due to the diffusion poles is shortened, while the opposite happens for the transmission poles (notice the different scales). See text for details.

type, but “explosive” in nature; now $\text{Im } s_n^{(t)} = 2\pi n / \delta$. (ii) The transmission poles have a very different dependence on the intensity of the interaction, Φ' : For a wide range of values for Φ' the characteristic times associated with the transmission poles remain essentially constant. We remark that the stability condition $\Phi' \leq 1$ is verified.

Figure 11 displays the power spectrum for the excitatory network. It is worth noting that in this case the “diffusion” part of the spectrum dominates over the “transmission” part. The positions of the peaks are the $\text{Im } s_n^{(t)}$ and $\text{Im } \lambda_n$ above.

Figure 10 further illustrates the characteristic times associated with the diffusion and the transmission poles. One distinctive feature of the excitatory case is the very strong dependence of the longest time scale (associated with $s_1^{(d)}$), on Φ' ; this point is further discussed in the following subsection.

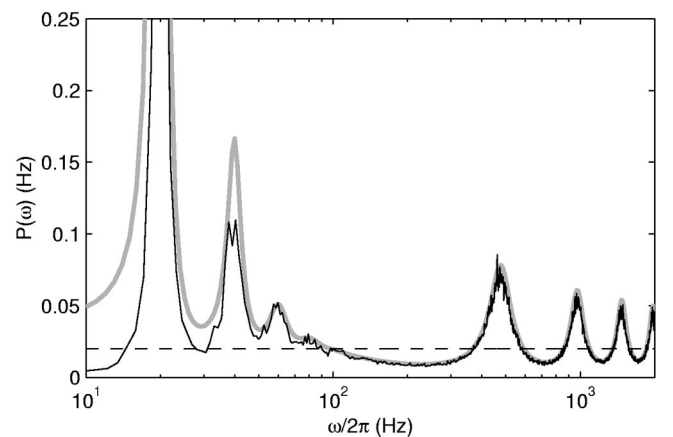


FIG. 11. Power spectrum of the activity of a population of coupled excitatory neurons in a drift-dominated regime: Simulations vs theory. The white noise variance ν_0/N is given by $\nu_0 = 20$ Hz and $N = 1000$. The coupling strength is such that $\Phi' = 0.6$.

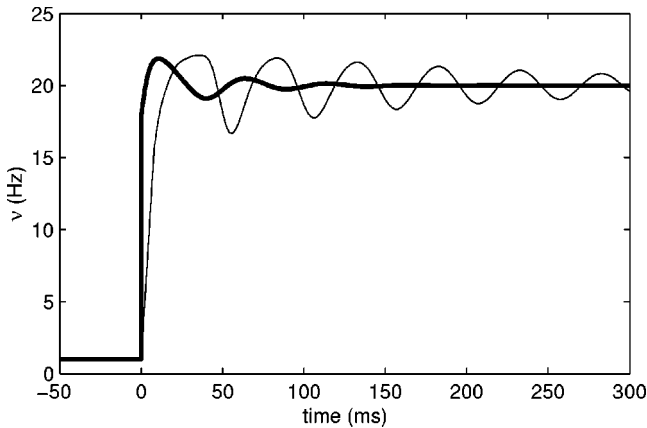


FIG. 12. Transient responses to a stepwise stimulation of an excitatory population, for two different coupling strengths. The network parameters are the same as two of the points in Figs. 9 and 10. The transient responses of a weakly coupled ($\Phi' = 0.6$, thin line) and a strongly interacting ($\Phi' = 0.95$, thick line) network are shown. Only the first four pairs of diffusion poles are used. The stimulation is given by an instantaneous increase of the emission rate of external neurons at $t = 0$. The steady states of the population before and after the stimulation are, respectively, 1 Hz and 20 Hz.

D. A possible effect of learning

Figure 12 shows the theoretical prediction for the transient response of an interacting excitatory population which, starting from a stable state of low emission rate (1 Hz in the case shown), undergoes a sudden jump in its external input, which is then kept constant, making the global activity of the network converge to a steady state of higher activity (20 Hz). For the same initial and final asymptotic average emission rate, we show in the figure how the value of Φ' affects the transient response: higher values of Φ' entail quicker response, and faster damping of the oscillations [42]. This is consistent with the stated dependence of $\text{Re } s_n^{(d)}$ on Φ' , and the fact that $s_n^{(d)}$ dominate the transient response.

For a given network architecture and neuron's parameters, increasing values of Φ' imply stronger recurrent couplings, as we expect to be brought about by a *learning* process (for example in a Hebbian learning scenario [43,44]). This effect could have deep functional implications, and we elaborate briefly on this point in Sec. IV.

The spectral analysis, shown in Fig. 13, illustrates how, besides the transient response, the effects of synaptic potentiation can be appreciated looking at the stationary activity state. In particular, it is seen that the value of Φ' essentially affects only the “diffusion” part of the spectrum, leaving the “transmission” part almost unchanged.

From Fig. 13 we also see that the $\omega = 0$ component is much higher for the higher value of Φ' . Since in general the height of each component in the spectrum is determined by the real part of the corresponding pole, again we see here a manifestation of the increasing Φ' bringing the network towards the stability boundary: The $s_0^{(t)}$ pole in fact, which gives a $\omega = 0$ contribution, is the one determining the stability of the network, and its real part is a decreasing function of Φ' , as we discussed in relation to Fig. 9.

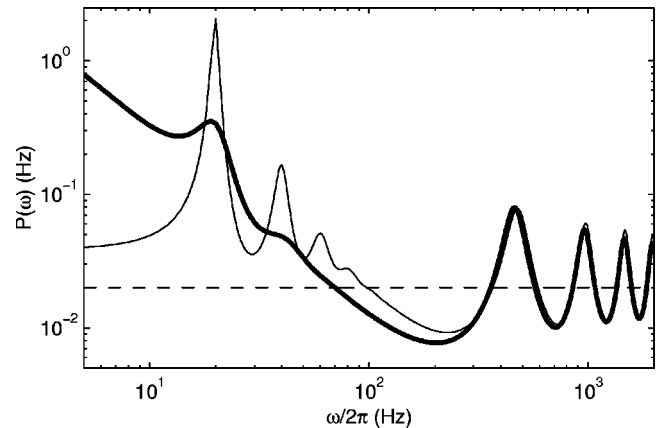


FIG. 13. Power spectrum of an excitatory population in a drift-dominated regime, for different coupling strengths. For the same network of Fig. 9, the power spectrum is shown for a weakly coupled ($\Phi' = 0.6$, thin line) and a strongly interacting ($\Phi' = 0.95$, thick line) network. The high-frequency part of the spectrum stays essentially unaffected, while the “diffusive,” low-frequency part shows appreciable changes. The white noise spectrum (dotted line) has variance ν_0/N given by $\nu_0 = 20$ Hz and $N = 1000$.

IV. DISCUSSION

The main purpose of the present work is to improve on some aspects of previous dynamical treatments of the population activity of a network of interacting neurons.

We focused on the asynchronous collective neural states; this is not unreasonable, in view of typical cortical conditions (particularly taking into account the ability of neural modules to quickly react to stimulation [15]). On the other hand, it would be desirable to extend the coverage of the dynamical scenarios offered here to other, globally stationary and/or nonstationary regimes, in the spirit of the “phase diagrams” derived in [7,9,13].

We expand a bit in the following on possible experimental implications of the spectral analysis of $\nu(t)$, comment on the mentioned “priming” effects related to synaptic modifications, and finally list some open problems.

A. Power spectrum and network properties

The predictions of the theory presented here about the power spectrum $P(\omega)$ of the collective activity, amenable in principle to experimental investigation, relate to quantities such as the (distribution of) delays (which could effectively embody the effects of slow synaptic currents [9]), or the pattern of synaptic couplings. One obvious difficulty in estimating the $P(\omega)$ is that one should be able to get a reliable estimate of the collective activity $\nu(t)$. An experimental measure of the characteristic times of the transient response of the network to abrupt variation in its inputs would provide an independent clue about essential features of the power spectrum (the diffusion poles). While such a measurement seems presently unfeasible *in vivo*, one can speculate on the possibility to perform it *in vitro*. Specifically, one could imagine performing a long series of stepwise stimulations of a small neural population in a slice (for example, using mul-

tielelectrode arrays), recording each time the activity of a small number of neurons; the set of multiple recordings (aligned in time) would provide an estimate of the transient $\nu(t)$ (such a pooling strategy was explored in Refs. [2,45] in a simple setting). Measuring the transient response this way could be much easier than trying to estimate the *stationary* network activity.

On the other hand, especially in view of the characterization of the spectral content of the neural activity recorded *in vivo*, it is tempting to consider the role of finite-size noise as a network's self-probing signal, such that the frequency response of the collective activity is exposed even in the absence of external stimulation tuned on purpose.

B. Priming effects induced by “learning”

We saw in simple cases how the characteristic times of the network response depend on the slope Φ' of the population gain function, and we mentioned that this can be viewed as a possible effect of “learning,” as long as the latter is described as a sequence of synaptic modifications, affecting in turn μ and σ^2 . This is relevant in view of a scenario in which, for example, a series of neuronal modules (say a processing chain from “sensory” to deeper areas) propagate information along the chain, in such a way as to reflect the “familiarity” or “novelty” of a stimulus (a familiar stimulus eliciting a quicker response).

As a qualitative indication of the possible link between successive stages of learning and the speed of the population response to external stimuli, we mention the results of Ref. [34], in which *in vivo* recording in behaving monkeys performing a delayed task showed a marked dependence of the latency of the response on the degree of “familiarity” of the stimuli. Figure 2C of Ref. [34] shows clearly that the response to novel stimuli (to which to apply the already learned task) drops after 200 trials to about 80% of its initial value. Though compatible with several possible explanations, such experimental evidence is suggestive of a possible direct implication of the average synaptic potentiation brought about by learning.

We remark that if one adopts a generic first-order dynamics for the rate ν , $\dot{\nu}=f(\nu)$ (see [5,6] for approaches of this type), given a fixed point ν_0 , such that $f(\nu_0)=0$, with stability condition $f'(\nu_0)<0$, it is easy to see that the relaxation time to ν_0 is $-1/f'(\nu_0)$, and the closer the system is to the stability boundary, the longer is the relaxation time. The opposite emerges from the present analysis. Whatever time scale is plugged into the above naive dynamics, the suggested relation with stability is misleading: coming close to the stability boundary in fact makes the network respond faster, while the stability condition itself is determined by poles whose typical characteristic times are much shorter, and do not essentially affect the transient response.

C. Some open issues

On the theoretical side, some important features are missing in the class of models considered in this work, and make the link with experimental findings still fleeting. One of these

is the variety of noninstantaneous synaptic transmission mechanisms of the presynaptic action potentials. Actually, synaptic interactions are mediated by the diffusion of neurotransmitters and the kinetics of post-synaptic receptors, whose time constants and dynamics are quite well established (see, for instance, Ref. [46]).

Indications about the role of synaptic currents were given in Refs. [5,6,15] for drift-dominated regimes.

In the mean-field framework, it has been suggested that synaptic time constants can be effectively considered as transmission delays: In Ref. [9], the effects of the characteristic time scale of the (inhibitory) synaptic current have been illustrated through a study of the network's state space.

Incorporating the effect of noninstantaneous synaptic currents has recently been the subject of several other efforts. In Ref. [38], following the approach pioneered in Ref. [5], a population density approach for the evolution of the $p(\nu, t)$ is complemented by a dynamic equation for the average (inhibitory) synaptic conductance (a mean-field treatment of the synaptic transmission). In Ref. [47], the population density approach is further extended to take into account both excitatory and inhibitory synaptic contributions, and the effects of their fluctuations, developing an effective dimensional reduction of the otherwise high-dimensional Fokker-Planck equation. Reference [48] addresses the noise-filtering properties of the IF neuron's output in connection with non-negligible (but small) synaptic time scales, and shows that finite synaptic times bring about quicker neuron response to transient changes in its input.

Much is still to be done in this respect, to characterize the behavior of the coupled network in different (especially noise-dominated) regimes. As part of work in progress, we plan to extend the approach described in the present paper to perturbatively take into account noninstantaneous synaptic currents [49].

The formalism illustrated in the present paper can in principle be applied to the widely used leaky IF neuron model. Such application would be interesting in several respects: It would provide a characterization of the phenomenology for the “default” model for biologically motivated modeling, making it easier to compare and contrast previous results. Besides, we formulated in the present paper some conjectures (such as the fact that the eigenvalues of the Fokker-Planck operator are purely real in noise-dominated regimes); it would be interesting to check their validity for the leaky IF neuron model.

Extending the treatment to the leaky IF neuron implies a technical complication, essentially due to the fact that the eigenvalues and eigenfunctions of the Fokker-Planck operator can only be expressed in terms of special functions (parabolic cylinder functions).

ACKNOWLEDGMENT

We gratefully acknowledge a very fruitful correspondence with W. Gerstner and N. Brunel. Thanks are due to A. Campa for stimulating discussions in the early stages of the work, and to S. Fusi and D. J. Amit for detailed comments on the manuscript.

- [1] A more complete historical account of the subject can be found, for example, in [7].
- [2] B. W. Knight, *J. Gen. Physiol.* **59**, 734 (1972).
- [3] H. R. Wilson and J. D. Cowan, *Biophys. J.* **12**, 1 (1972).
- [4] D. J. Amit and M. Tsodyks, *Network* **2**, 259 (1991).
- [5] A. Treves, *Network* **4**, 259 (1993).
- [6] L. F. Abbott and C. van Vreeswijk, *Phys. Rev. E* **48**, 1483 (1993).
- [7] W. Gerstner, *Phys. Rev. E* **51**, 738 (1995).
- [8] D. J. Amit and N. Brunel, *Cereb. Cortex* **7**, 237 (1997a).
- [9] N. Brunel and V. Hakim, *Neural Comput.* **11**, 1621 (1999).
- [10] M. Spiridon and W. Gerstner, *Network* **10**, 257 (1999).
- [11] B. W. Knight, D. Manin, and L. Sirovich, in *Proceedings of Symposium on Robotics and Cybernetics, Lille-France, July 9-12*, edited by E. C. Gerf (1996).
- [12] S. Fusi and M. Mattia, *Neural Comput.* **11**, 633 (1999).
- [13] N. Brunel, *J. Comput. Neurosci.* **8**, 183 (2000).
- [14] M. Tsodyks and T. Sejnowsky, *Network* **6**, 111 (1995).
- [15] W. Gerstner, *Neural Comput.* **12**, 43 (2000).
- [16] S. Thorpe, D. Fize, and C. Marlot, *Nature (London)* **381**, 520 (1996).
- [17] D. Q. Nykamp and D. Tranchina, *J. Comput. Neurosci.* **8**, 19 (2000).
- [18] Conditions favoring independence are sparse connectivity, a random distribution of synaptic efficacies which can compensate for sparseness when connectivity is high or, in general, a suitable source of quenched randomness affecting the communication among the neurons.
- [19] H. Risken, *The Fokker-Planck Equation: Methods of Solution and Applications* (Springer-Verlag, Berlin, 1984).
- [20] We remark that in deriving the above Fokker-Planck equation in the general case (2.2) of a multiplicative noise, the condition $\langle g(V,t)\Gamma(t) \rangle = 0$ plays a crucial role, since if the latter condition is not fulfilled, a further, “noise-induced” drift appears in the A coefficient of the Fokker-Planck equation.
- [21] L. Sirovich, A. Omurtag, and B. W. Knight, *SIAM (Soc. Ind. Appl. Math.) J. Appl. Math.* **60**, 2009 (2000).
- [22] B. W. Knight, *Neural Comput.* **12**, 473 (2000).
- [23] C. van Vreeswijk and H. Sompolinsky, *Science* **274**, 1724 (1996).
- [24] The ratio between the standard deviation and the mean of the interspike intervals.
- [25] The irrelevance of the detailed statistics of the interspike intervals for the collective dynamics of the network has been recognized in a different context in [50].
- [26] In Ref. [19] it is suggested (for a slightly different expansion strategy) that this is indeed the case when the terms A and B in the Fokker-Planck equation are rational functions of v (see [11] for an explicit example).
- [27] Not to be individually considered as probability currents, since the ϕ_n 's are not individually probability density functions.
- [28] As noted by several authors, the above definition of ν is free from the difficulties that arise in the definition based on taking averages of single spike trains over small time intervals.
- [29] Indeed, the $(e^\delta - 1)\Phi' \nu_1(0)/s$ term is finite in the potentially dangerous limit $s \rightarrow 0$, and the singularities possibly arising from the term in the numerator involving $(s\mathbf{I} - \mathbf{\Lambda})^{-1}$ are eliminated by the analogous term in the denominator.
- [30] While the stability condition $\Phi' < 1$ appears superficially consistent with general and standard arguments, it applies to a special case (see below for other examples). Besides, we argue in Sec. IV that simple arguments appropriate for a *first-order* dynamics lead to wrong conclusions in the case under study.
- [31] G. Mongillo and D. J. Amit, *J. Comput. Neurosci.* **11**, 249 (2001).
- [32] A pole near one of the eigenvalues of L , driving the instability of the network for small σ^2 (which our analysis proves to be a special, large δ effect) had been predicted in Ref. [22] to be a general property, on the basis of what appears as an unwarranted condition imposed on the poles near λ_n .
- [33] H. C. Tuckwell, *Introduction to Theoretical Neurobiology* (Cambridge University Press, Cambridge, England, 1988), Vol. 2.
- [34] C. A. Erickson and R. Desimone, *J. Neurosci.* **19**, 10404 (1999).
- [35] We mention for completeness that in the small- σ^2 limit, in the drift-dominated regime the eigenvalues (therefore, in most conditions, the diffusion poles) have a real part $\sim \sigma^2$, such that as $\sigma \rightarrow 0$ the diffusion poles bring about a marginal stability. See also [6] and [22] for a discussion of the eigenvalues of L in the limit of small σ^2 .
- [36] For example, for the extreme case of full connectivity, with all synapses chosen as random variables drawn from the same probability distribution, the afferent currents to two generic neurons are determined by the convolution of the same realization of a stochastic point process (the common sequence of afferent spikes) with two *independent* realizations of the process generating the synaptic couplings.
- [37] D. J. Amit and N. Brunel, *Network* **8**, 373 (1997b).
- [38] D. Q. Nykamp and D. Tranchina, *Neural Comput.* **13**, 511 (2001).
- [39] P. Dayan and L. F. Abbott, *Theoretical Neuroscience* (MIT Press, Cambridge, MA, 2001).
- [40] W. Gerstner and W. Kistler, *Spiking Neuron Models* (Cambridge University Press, Cambridge, England, 2002).
- [41] D. J. Mar *et al.*, *Proc. Natl. Acad. Sci. U.S.A.* **96**, 10450 (1999).
- [42] It is clear from the above discussion that the characteristic times of the population are not directly determined by single neuron properties such as the membrane time constant.
- [43] D. J. Amit, *Behav. Brain Sci.* **18**, 617 (1995).
- [44] P. Del Giudice and M. Mattia, in *Neurocomputing—Computational Neuroscience: Trends in Research 2001*, edited by J. Bower (Elsevier Science, Amsterdam, 2001), Vols. 38–40, pp. 1175–1180.
- [45] B. W. Knight, *J. Gen. Physiol.* **59**, 767 (1972).
- [46] A. Destexhe, Z. F. Mainen, and T. J. Sejnowski, in *Methods in Neuronal Modeling*, edited by C. Koch and I. Segev (MIT Press, Cambridge, MA, 1998), pp. 1–25.
- [47] E. Haskell, D. Q. Nykamp, and D. Tranchina, *Network* **12**, 141 (2001).
- [48] N. Brunel, F. S. Chance, N. Fourcaud, and L. F. Abbott, *Phys. Rev. Lett.* **86**, 2186 (2001).
- [49] Previous attempts within the diffusion approximation are reported in [9]. [47] takes into account the higher-order contributions in the Kramers-Moyal expansion.
- [50] W. Gerstner and J. L. van Hemmen, *Biol. Cybern.* **67**, 195 (1992).